Article

Acrylonitrile Insertion Reactions of Cationic Palladium Alkyl Complexes

Fan Wu, Stephen R. Foley, Christopher T. Burns, and Richard F. Jordan

J. Am. Chem. Soc., **2005**, 127 (6), 1841-1853• DOI: 10.1021/ja044122t • Publication Date (Web): 25 January 2005

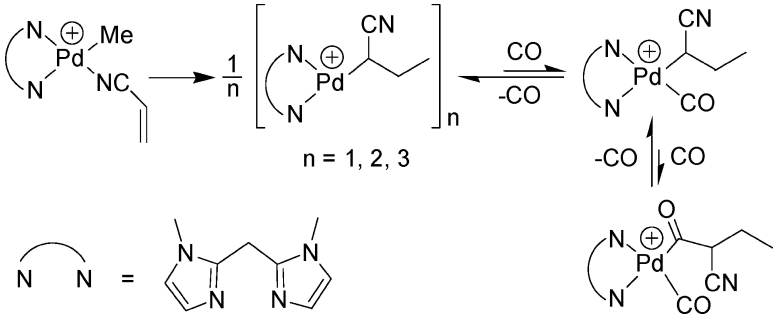

More About This Article

Additional resources and features associated with this article are available within the HTML version:

- Supporting Information
- Links to the 11 articles that cite this article, as of the time of this article download
- Access to high resolution figures
- Links to articles and content related to this article
- Copyright permission to reproduce figures and/or text from this article

View the Full Text HTML

J|A|C|S
ARTICLES
Published on Web 01/25/2005

Acrylonitrile Insertion Reactions of Cationic Palladium Alkyl Complexes

Fan Wu, Stephen R. Foley, Christopher T. Burns, and Richard F. Jordan*

Contribution from the Department of Chemistry, The University of Chicago, 5735 South Ellis Avenue, Chicago, Illinois, 60637

Received September 27, 2004; E-mail: rfjordan@uchicago.edu

Abstract: The reactions of acrylonitrile (AN) with "L_2PdMe^+" species were investigated; (L_2 = CH_2(*N*-Me-imidazol-2-yl)$_2$ (**a**, bim), (*p*-tolyl)$_3$CCH(*N*-Me-imidazol-2-yl)$_2$ (**b**, Tbim), CH_2(5-Me-2-pyridyl)$_2$ (**c**, CH_2py′$_2$), 4,4′-Me_2-2,2′-bipyridine (**d**), 4,4′-^{t}Bu$_2$-2,2′-bipyridine (**e**), (2,6-^{i}Pr$_2$−C_6H_3)N=CMeCMe=N(2,6-^{i}Pr$_2$−C_6H_3) (**f**)). [L_2PdMe(NMe$_2$Ph)][B(C_6F_5)$_4$] (**2a**−**c**) and [{L_2PdMe}$_2$(μ-Cl)][B(C_6F_5)$_4$] (**2d**−**f**) react with AN to form N-bound adducts L_2Pd(Me)(NCCH=CH_2)$^+$ (**3a**−**f**). **3a**−**e** undergo 2,1 insertion to yield L_2Pd{CH(CN)Et}$^+$, which form aggregates [L_2Pd{CH(CN)Et}]$_n^{n+}$ (n = 1−3, **4a**−**e**) in which the Pd units are proposed to be linked by PdCHEtCN- - -Pd bridges. **3f** does not insert AN at 23 °C. **4a**−**e** were characterized by NMR, ESI-MS, IR and derivatization to L_2Pd{CH(CN)Et}(PR_3)$^+$ (R = Ph (**5a**−**e**), Me (**6a**−**c**)). **4a**,**b** react with CO to form L_2Pd{CH(CN)Et}(CO)$^+$ (**7a**,**b**). **7a** reacts with CO by slow reversible insertion to yield (bim)Pd{C(=O)CH(CN)Et}(CO)$^+$ (**8a**). **4a**−**e** do not react with ethylene. (Tbim)PdMe$^+$ coordinates AN more weakly than ethylene, and AN insertion of **3b** is slower than ethylene insertion of (Tbim)Pd(Me)(CH_2=CH_2)$^+$ (**10b**). These results show that most important obstacles to insertion polymerization or copolymerization of AN using L_2PdR$^+$ catalysts are the tendency of L_2Pd{CH(CN)CH_2R}$^+$ species to aggregate, which competes with monomer coordination, and the low insertion reactivity of L_2Pd{CH(CN)CH_2R}(substrate)$^+$ species.

Introduction

Acrylonitrile (AN) homopolymers and copolymers and their derivatives possess unique properties that are exploited in acrylic fibers, nitrile rubbers, and other applications.[1] Polyacrylonitrile (PAN) and ethylene/AN copolymers are prepared commercially by radical polymerization, and PAN can also be prepared by anionic polymerization. The synthesis of AN polymers by insertion polymerization using metal catalysts is an attractive goal, because, as in conventional olefin polymerization, tuning of the catalyst structure may enable greater control over polymer structures and properties than is possible with radical or anionic polymerization.[2,3]

A general scheme for the possible insertion polymerization or copolymerization of AN is shown in Scheme 1. Several challenges are immediately apparent. First, AN can coordinate to metals through either the CN group or the C=C unit, or by several bridging modes.[4−6] Insertion polymerization catalysts

Scheme 1

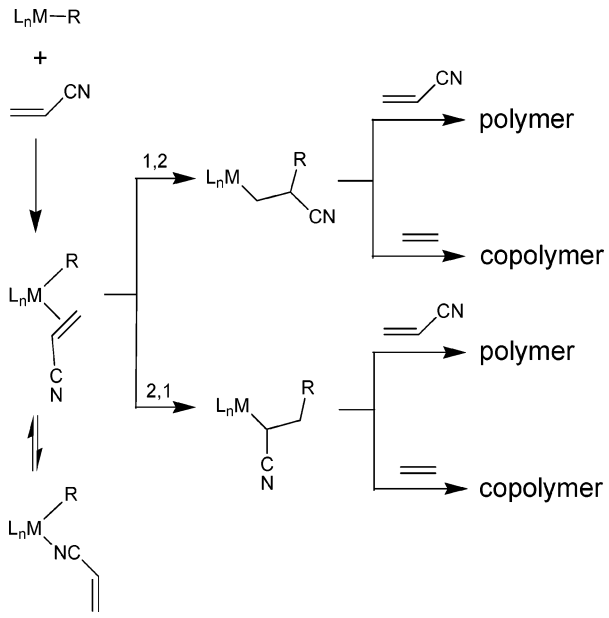

normally contain high valent, poor-back-bonding metal centers, for which the N-bound mode will be favored. For example, an N-bound AN ligand is present in the platinum α-diimine complex (ArN=CHCH=NAr)Pt(Me)(NCCH=CH_2)$^+$ (Ar = 2-OSi^{i}Pr$_3$-6-Me−C_6H_3),[4a] which is an analogue of the classic {(2,6-^{i}Pr$_2$−C_6H_3)N=CMeCMe=N(2,6-^{i}Pr$_2$−C_6H_3)}-PdMe(L)$^+$ catalyst.[7] The requirement for N/π isomerization will increase the overall insertion barrier in such cases. N/π-

(1) (a) Acrylonitrile and Acrylonitrile Polymers. In *Kirk-Othmer Encyclopedia of Chemical Technology*, 3rd ed.; Wiley & Sons: New York, 1983; Vol. 1, pp 414−456. (b) Kirk-Othmer Encyclopedia of Chemical Technology Home Page. http://www.mrw.interscience.wiley.com/kirk/ (accessed June 2003). (c) Alger, M. *Polymer Science Dictionary*, 2nd ed.; Chapman Hall: New York, 1997; pp 6−7.
(2) Boffa, L. S.; Novak, B. M. *Chem. Rev.* **2000**, *100*, 1479.
(3) Ittel, S. D.; Johnson, L. K.; Brookhart, M. *Chem. Rev.* **2000**, *100*, 1169.
(4) For representative N-bound AN complexes, see: (a) Albietz, P. J., Jr.; Yang, K.; Lachicotte, R. J.; Eisenberg, R. *Organometallics* **2000**, *19*, 3543. (b) Yang, Z.; Ebihara, M.; Kawamura, T. *J. Mol. Catal. A: Chemical* **2000**, *158*, 509. (c) Chin, C. K.; Chong, D.; Lee, S.; Park, Y. J. *Organometallics*, **2000**, *19*, 4043. (d) Davidson, J. L.; Ritchtzenhein, H.; Thiebaut, B. J. S.; Landskron, K.; Rosair, G. M. *J. Organomet. Chem.* **1999**, *592*, 168. (e) Fischer H.; Roth, G.; Reindl, D.; Troll, C. *J. Organomet. Chem.* **1993**, *454*, 133.

isomerization was observed for $CpFe(CO)_2(AN)^+$.[8] Nitriles are known to inhibit ethylene polymerization by α-diimine catalysts.[3]

Assuming that the C═C π complex can be accessed, AN insertion can occur with either 1,2 or 2,1 regiochemistry to yield $L_nMCH_2CH(CN)R$ or $L_nMCH(CN)CH_2R$ products, respectively. Several examples of 2,1 AN insertion into L_nM-H bonds are known.[9] For example, $(Me_2NCS_2)Pd(PEt_3)H$ reacts with AN at low temperature to yield $(Me_2NCS_2)Pd(PEt_3)\{CH(CN)Me\}$.[9a] Several examples of net 1,2 additions of L_nM-H species to the C═C bond of AN have been reported, which are believed to proceed by radical mechanisms.[10] Examples of net 2,1 AN insertion into Pt-amido and Pt-phosphido bonds have also been reported.[11] AN insertions into metal-alkyl bonds have been proposed as key steps in Ru-catalyzed AN dimerization, metal-mediated coupling reactions involving AN, and other reactions, but have not been directly observed to date.[12]

Numerous metal complexes have been reported to polymerize AN.[13] While it is likely that in most of these cases the polymerization mechanism is either anionic or radical, few systems have been studied in detail. For example, Cy_3PCuMe and $(bipy)_2FeEt_2$ each initiate the anionic polymerization of AN.[13j−o] The major initiator in AN polymerization by Cy_3PCuMe is PCy_3, which is liberated from the Cu complex.[14a] A transient iron hydride complex formed by β-H elimination of $(bipy)_2FeEt_2$ was proposed to initiate AN polymerization by $(bipy)_2FeEt_2$.[14a] Evidence for radical polymerization of AN by $(bipy)_2FeEt_2$ has also been reported.[14b]

To identify and understand the chemical issues that underlie the challenge of achieving metal-mediated AN insertion polymerization, we are investigating the reactions of single-site olefin polymerization catalysts with this substrate. Here we describe studies of the reactions of representative cationic Pd(II) ethylene dimerization and polymerization catalysts with AN. Parallel studies of the reactions of neutral and anionic Pd(II) alkyl complexes with AN by Piers and co-workers are described in a companion paper.[15]

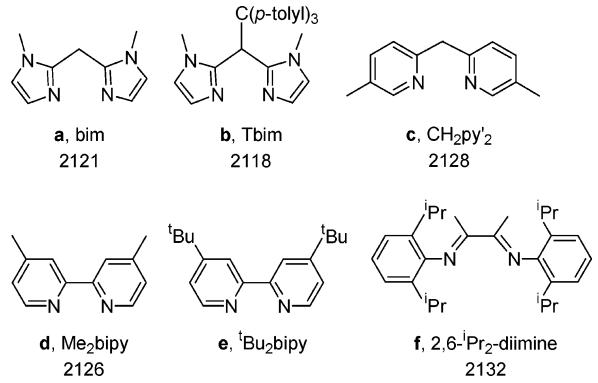

Figure 1. Ancillary ligands (L_2) used in this work and ν_{CO} values (in cm^{-1}) for the terminal CO ligands in the corresponding $L_2Pd\{C(=O)Me\}(CO)^+$ complexes.

Results

Choice of Probe Complexes. Six representative "$L_2PdCH_3^+$" catalysts, which contain the bidentate nitrogen L_2 ligands **a**−**f** in Figure 1, were studied in this work.[16] Cationic "L_2PdMe^+" species were generated as $[L_2PdMe(NMe_2Ph)][B(C_6F_5)_4]$ (**2a**−**c**) or $[\{L_2PdMe\}_2(\mu\text{-Cl})][B(C_6F_5)_4]$ (**2d**−**f**) complexes as described below. Ligands **a**−**f** were chosen to enable investigation of how the electronic and steric properties of L_2PdMe^+ species influence their reactivity with AN. The electrophilic character of L_2PdMe^+ species is expected to vary in the order **a**,**b** < **c**,**d**,**e** < **f**, based on the ν_{CO} values for the terminal CO ligands in the corresponding $L_2Pd\{C(=O)Me\}(CO)^+$ complexes, which are listed in Figure 1.[17] Ligands **b** and **f** are sterically bulky while **a** and **c**−**e** are not. $L_2PdMe(ethylene)^+$ species based on these ligands catalyze the dimerization (**a**, **c**−**e**) or polymerization (**b**, **f**) of ethylene.[7,17] The ethylene insertion rates of $L_2PdMe(ethylene)^+$ species increase with increasing steric crowding and electrophilic character at Pd (**a** < **b** < **c** ≪ **f**).[7,17]

(5) For representative C═C-π-bonded AN complexes see (a) Río, I. D.; Gossage, R. A.; Hannu, M. S.; Lutz, M.; Spek, A. L.; Koten, G. V. *Organometallics* **1999**, *18*, 1097. (b) Maekawa, M.; Munakata, M.; Kuroda-Sowa, T.; Hachiya, K. *Inorg. Chim. Acta* **1994**, *227*, 137. (c) Felice, V. D.; Albano, V. G.; Castellari, C.; Cucciolito, M. E.; Renzi, A. D. *J. Organomet. Chem.* **1991**, *403*, 269. (d) Albano, V. G.; Castellari, C.; Cucciolito, M. E.; Panunzi, A.; Vitagliano, A. *Organometallics* **1990**, *9*, 1269. (e) Tolman, C. A.; Seidel, W. C. *J. Am. Chem. Soc.* **1974**, *96*, 2774.
(6) Bryan, S. J.; Huggett, P. G.; Wade, K.; Daniels, J. A.; Jennings, J. R. *Coord. Chem. Rev.* **1982**, *44*, 149.
(7) (a) Brookhart, M.; Leatherman, M. D.; Liu, W.; Williams, B. S. *Polym. Mater. Sci. Eng.* **2004**, *90*, 79. (b) Shultz, L. H.; Tempel, D. J.; Brookhart, M. *J. Am. Chem. Soc.* **2001**, 123, 11539. (c) Gottfried, A. C.; Brookhart, M. *Macromolecules* **2001**, *34*, 1140. (d) Tempel, D. J.; Johnson, L. K.; Huff, R. L.; White, P. S.; Brookhart, M. *J. Am. Chem. Soc.* **2000**, *122*, 6686. (e) Johnson, L. K.; Killian, C. M.; Brookhart, M. *J. Am. Chem. Soc.* **1995**, *117*, 6414.
(8) Rosenblum, M.; Turnbull, M. M.; Begum, M. K. *J. Organomet. Chem.* **1987**, *321*, 67.
(9) (a) Reger, D. L.; Garza, D. G. *Organometallics* **1993**, *12*, 554. (b) Herberich, G. E.; Barlage, W.; Linn, K. *J. Organomet. Chem.* **1991**, *414*, 193. (c) Deshpande, S. S.; Gopinathan, S.; Gopinathan, C. *J. Organomet. Chem.* **1989**, *378*, 103. (d) Gopinathan, S.; Unni, I. R.; Gopinathan, C. *Polyhedron* **1986**, *5*, 1921. (e) Otsuka, S.; Nakamura, A. *J. Am. Chem. Soc.* **1972**, *94*, 1886.
(10) (a) Anderson, D. J.; Eisenberg, R. *Organometallics* **1996**, *15*, 1697. (b) Baddley, W. H.; Fraser, M. S. *J. Am. Chem. Soc.* **1969**, *91*, 3661. (c) Lemsink, A. J.; Noltes, J. G. *Tetrahedron Lett.* **1966**, 335.
(11) (a) Seul, J. M.; Park, S. *J. Chem. Soc., Dalton Trans.* **2002**, *6*, 1153. (b) Park, S. *Bull. Korean Chem. Soc.* **2001**, *22*, 15. (c) Wicht, D. K.; Kovacik, I.; Glueck, D. S.; Liable-Sands, L. M.; Incarvito, C. D.; Rheingold, A. L. *Organometallics* **1999**, *18*, 5141. (d) Wicht, D. K.; Kourkine, I. V.; Lew, B. M.; Nthenge, J. M.; Glueck, D. S. *J. Am. Chem. Soc.* **1997**, *119*, 5039. (e) Cowan, R. L.; Trogler, W. C. *J. Am. Chem. Soc.* **1989**, *111*, 4750. (f) Cowan, R. L.; Trogler, W. C. *Organometallics* **1987**, *6*, 2451.
(12) (a) Yi, C. S.; Torres-Lubian, J. R.; Liu, N.; Rheingold, A. L.; Guzei, I. A. *Organometallics* **1998**, *17*, 1257. (b) Depree, G. J.; Main, L.; Nicholson, B. K. *J. Organomet. Chem.* **1998**, *155*, 281. (c) Janecki, T.; Pauson, P. L.; Pietrzykowski, A. *J. Organomet. Chem.* **1987**, *325*, 247. (d) Bryndza, H. E.; Calabrese, J. C.; Wreford, S. S. *Organometallics* **1984**, *3*, 1603. (e) Healy, K. P.; Pletcher, D. *J. Organomet. Chem.* **1978**, *161*, 109. (f) Cooke, M. P., Jr.; Parlman, R. M. *J. Am. Chem. Soc.* **1977**, *99*, 5222. (g) Otsuka, S.; Nakamura, A.; Yoshida, T.; Naruto, M.; Ataka, K. *J. Am. Chem. Soc.* **1973**, *95*, 3180. (h) Fukuoka, A.; Nagano, T.; Furuta, S.; Yoshizawa, M.; Hirano, M.; Komiya, S. *Bull. Chem. Soc. Jpn.* **1998**, *71*, 1409.
(13) (a) Jenkins, A. D.; Lappert, M. F.; Srivastava, R. C. *Polymer Lett.* **1968**, *6*, 865. (b) Saegusa, T.; Horiguchi, S.; Tsuda, T. *Macromolecules* **1975**, *8*, 112. (c) Gandhi, V. G.; Sivaram, S.; Bhardwaj, I. S. *J. Macromol. Sci., Chem.* **1983**, *A19*, 147. (d) Billingham, N. C.; Lees, P. D. *Makromol. Chem.* **1993**, *194*, 1445. (e) Tsuchhara, K.; Suzuki, Y.; Asai, M.; Soga, K. *Chem. Lett.* **1999**, 891. (f) Siemeling, U.; Kölling, L.; Stammler, A.; Stammler, H.-G.; Kaminski E.; Fink, G. *Chem. Commun.* **2001**, 1177. (g) Suh, M. P.; Oh, Y.; Kwak, C. *Organometallics* **1987**, *6*, 411. (h) Mudalige, D. C.; Rempel, G. L. *J. Macromol. Sci., Chem.* **1997**, *A34*, 361. (i) Arndt, S.; Beckerle, K.; Hultzsch, K. C.; Spaniol, T. P.; Okuda, J. *J. Mol. Catal. A: Chem.* **2002**, *190*, 215. (j) Yamamoto, A.; Ikeda, S. *J. Am. Chem. Soc.* **1967**, *89*, 5989. (k) Ikariya, T.; Yamamoto, A. *J. Organomet. Chem.* **1974**, *72*, 145. (l) Miyashita, A.; Yamamoto, T.; Yamamoto, A. *Bull. Chem. Soc. Jpn.* **1977**, *50*, 1109. (m) Yamamoto, T.; Yamamoto, A.; Ikeda, S. *Bull. Chem. Soc. Jpn.* **1972**, *45*, 1111. (n) Yamamoto, T.; Yamamoto, A.; Ikeda, S. *Bull. Chem. Soc. Jpn.* **1972**, *45*, 1104. (o) Yamamoto, A. *J. Chem. Soc., Dalton Trans.* **1999**, *7*, 1027.
(14) (a) Schaper, F.; Foley, S. R.; Jordan, R. F. *J. Am. Chem. Soc.* **2004**, *126*, 2114. (b) Yang, P.; Chan, B. C. K., Baird, M. C. *Organometallics* **2004**, *23*, 2752.
(15) Groux, L. F.; Weiss, T.; Reddy, D. N.; Chase, P. A.; Piers, W. E.; Ziegler, T.; Parvez, M.; Benet-Buchholz, J. *J. Am. Chem. Soc.* **2005**, *127*, 1854.
(16) L_2 = CH_2(*N*-Me-imidazol-2-yl)$_2$ (**a**, bim), (*p*-tolyl)$_3$CCH(*N*-Me-imidazol-2-yl)$_2$ (**b**, Tbim), CH_2(5-Me-2-pyridyl)$_2$ (**c**, $CH_2py'_2$), 4, 4′-Me_2-2, 2′-bipyridine (**d**, Me_2bipy), 4, 4′-$^tBu_2$-2, 2′-bipyridine (**e**, $^tBu_2$bipy), and (2, 6-$^iPr_2$−C_6H_3)N═CMeCMe═N(2, 6-$^iPr_2$−C_6H_3) (**f**, 2, 6-$^iPr_2$-diimine).
(17) Burns, C. T.; Jordan, R. F. *Abstracts of Papers, 224th ACS National Meeting, Boston*, **2002**, INOR-322.

Generation of $L_2PdMe(NMe_2Ph)^+$ and $[\{L_2PdMe\}_2(\mu\text{-}Cl)]^+$ Species. The reaction of L_2PdMe_2 (**1a**−**c**) with $[HNMe_2Ph][B(C_6F_5)_4]$ quantitatively generates $L_2PdMe(NMe_2Ph)^+$ (**2a**−**c**) and methane within 10 min at −78 °C (eq 1). The NMR spectra of **2a**−**c** show the presence of an unsymmetrical L_2 ligand and a NMe_2Ph ligand. Complexes **2a**−**c** are stable at −40 °C in CD_2Cl_2 but decompose to Pd^0 at 23 °C (significant Pd^0 observed within 10 min).

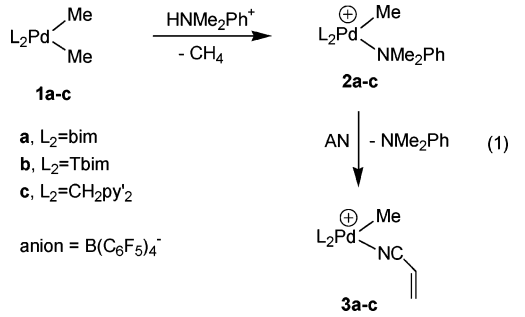

The chloride complexes $L_2PdMeCl$ (**1d**−**f**) were used as precursors to L_2PdMe^+ species because they are more stable than the corresponding L_2PdMe_2 compounds. The reaction of **1d**−**f** with 0.5 equiv of $[Li(Et_2O)_{2.8}][B(C_6F_5)_4]$ yields dinuclear $[\{L_2PdMe\}_2(\mu\text{-Cl})]^+$ complexes **2d**−**f** quantitatively (eq 2).[7d,18] Complexes **2d**−**f** are stable at 23 °C for several hours.

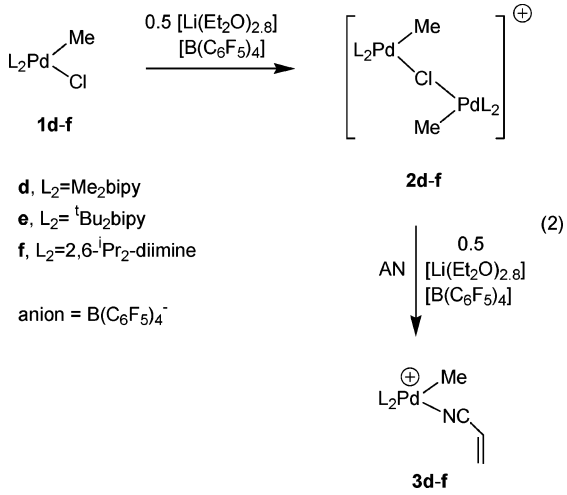

Generation of N-Bound $L_2Pd(Me)(NCCH{=}CH_2)^+$ Complexes (3a−f). Addition of excess AN to **2a**-**c** results in quantitative displacement of NMe_2Ph and formation of $L_2Pd(Me)(NCCH{=}CH_2)^+$ complexes (**3a**−**c**, eq 1). **2a** and **2c** react with AN at −60 °C within 5 min. In contrast, **2b** requires a higher temperature (−30 °C) and longer reaction time (30 min) for complete displacement to occur due to the presence of the bulky apical $C(p\text{-tolyl})_3$ substituent, which retards associative substitution processes. Similarly, AN adducts **3d**−**f** are generated quantitatively (5 min, 23 °C) by reaction of **2d**−**f** with excess AN in the presence of 0.5 equiv $[Li(Et_2O)_{2.8}][B(C_6F_5)_4]$ (eq 2).

The ^1H and ^{13}C NMR AN resonances of **3a**−**f** are only slightly shifted from the free AN positions. For example, the ^1H NMR AN resonances for **3a** (−60 °C) appear at δ 6.55 (d, J = 18, 1H, H_{trans}), 6.43 (d, J = 12, 1H, H_{cis}) and 5.93 (dd, J = 18, 12; 1H, H_{int}), ca. 0.3 ppm downfield from the corresponding free AN resonances. The ^{13}C NMR AN resonances of **3a** appear at δ 143.0 (C_{ter}), 119.2 (CN) and 105.7 (C_{int}), within 5 ppm of the corresponding free AN positions. Additionally, the IR υ_{CN} values of two representative examples, **3a** (2244 cm^{-1}) and **3d** (2247 cm^{-1}) are ca. 15 cm^{-1} higher than that for free AN (2230 cm^{-1}). These data are similar to data for known N-bound AN complexes, such as $(C_5Me_5)Ir(\eta^3\text{-}CHPhCHCH_2)(NCC{=}CH_2)^+$ (^1H NMR: δ 6.56−6.35 (m); ^{13}C NMR δ 143.4 (C_{ter}), 120.4 (CN) and 106.2 (C_{int}); υ_{CN} 2259 cm^{-1}), which was characterized by X-ray diffraction.[4c,6] In contrast, for C=C π-bound AN complexes, the ^1H and ^{13}C NMR AN resonances are normally shifted far upfield, and υ_{CN} is decreased, compared to the free AN values.[5,6] Therefore, it is clear that **3a**−**f** contain N-bound AN ligands. The presence of AN was confirmed by the ESI mass spectra of **3d** and **3f**, in which the $L_2Pd(Me)(AN)^+$ ions are the major cations observed.

Scheme 2

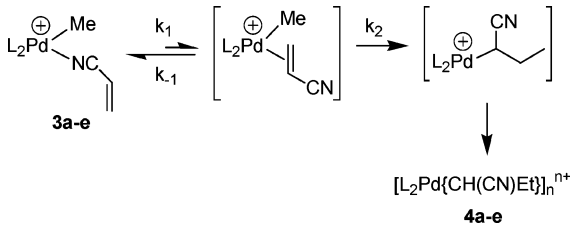

Acrylonitrile Insertion of 3a−e and Generation of $[L_2Pd\{CH(CN)Et\}]_n^{n+}$ Species (4a−e). Complexes **3a**−**e** undergo 2,1 insertion of the AN C=C bond at 23 °C to afford $L_2Pd\{CH(CN)Et\}^+$ products, which are formed as mixtures of $[L_2Pd\{CH(CN)Et\}]_n^{n+}$ aggregate species (**4a**−**e**, Scheme 2). ^1H NMR monitoring experiments show that **3a**−**e** are completely consumed but no free AN is consumed in this reaction. No intermediates in the conversion **3a**−**e** to **4a**−**e** were observed by NMR. In contrast, **3f** is stable at 23 °C for several days, and there is no evidence for AN insertion in this case under these conditions. The qualitative rates of AN insertion of **3a**−**e** to yield **4a**−**e**, as assessed by NMR monitoring of the disappearance of the Pd-Me resonance at 23 °C, vary in the order: **3b** ($t_{1/2}$ ca. 6 min) > **3a** ($t_{1/2}$ ca. 1.5 h), **3c**,**d** ($t_{1/2}$ ca. 4 h) > **3f** (no reaction).

The NMR spectra of **4a**−**e** are complex and show that several chemically inequivalent $[L_2PdCH(CN)Et]^+$ units are present in each case. For example, the ^1H NMR spectrum of **4a** contains three major sets of bim resonances implying the presence of three inequivalent unsymmetrical (bim)Pd environments. This spectrum also contains multiplets at δ 2.49 (1H), 2.22−1.78 (2H), 1.24−1.15 (3H) consistent with the presence of several inequivalent −CH(CN)Et units. The ESI mass spectra of several examples (**4a**−**c**) show the presence of $[L_2Pd\{CH(CN)Et\}]_n^{n+}$ ions (n = 1−3). For example, three major cations are observed in the ESI−MS of **4a**, with molecular weights and isotope patterns corresponding to $(bim)Pd\{CH(CN)Et\}^+$, $[(bim)Pd\{CH(CN)Et\}]_2^{2+}$ and $\{[(bim)Pd\{CH(CN)Et\}]_3^{3+}[B(C_6F_5)_4^-]\}$. While the detailed structures of **4a**−**e** have not been established, it is likely that the Pd units are linked by μ^2-*C,N*−PdCHEtCN- - -Pd bridges. The IR υ_{CN} bands for two representative cases, **4a** (2246 cm^{-1}) and **4d** (2249 cm^{-1}), appear at slightly higher frequency than those of free nitriles (e.g., $CH_3CH(CN)Et$, 2238

(18) Shen, H.; Jordan, R. F. *Organometallics* **2003**, *22*, 1878.

cm^{-1}).[19] These values are similar to υ_{CN} values for the μ^2-*C*,*N* α-cyanoalkyl complexes $[Pd_2(C_6F_5)_4\{\mu^2\text{-}C,N\text{-}CHXCN\}_2]^{2-}$ (X = CN, 2250 cm^{-1}; X = CO_2Me, 2240 cm^{-1}).[20] The υ_{CN} values in such systems reflect the compensating effects of the presence of the metal at C_α, which will reduce υ_{CN}, and coordination of the metal at the CN nitrogen, which will increase υ_{CN}.[21] Compounds **4a**−**e** are stable in CD_2Cl_2 solution at 23 °C for at least 10 days.

Although attempts to isolate **4a**−**e** using $B(C_6F_5)_4^-$ as the counterion were unsuccessful, $[(Me_2bipy)Pd\{CH(CN)Et\}]_n^{n+}$ was isolated as the $B\{3,5\text{-}(CF_3)_2\text{−}C_6H_3\}_4^-$ salt. The reaction of **1d** with 1 equiv of $Na[B\{3,5\text{-}(CF_3)_2\text{−}C_6H_3\}_4]$ and 10 equiv of AN in CH_2Cl_2 affords analytically pure $[(Me_2bipy)Pd\{CH(CN)Et\}][B\{3,5\text{-}(CF_3)_2\text{−}C_6H_3\}_4]$ (**4d′**) as a yellow solid (81%). The NMR spectra of **4d′** are very similar to those of **4d** (with the exception of the anion resonances) indicating that the aggregation of the two species is similar. Further support for the formulation of **4a**−**e** as 2,1 insertion products is provided by chemical derivatization experiments as discussed below.

Similar 2,1 AN insertion and aggregation by μ^2-*C*,*N*−PdCHEtCN- - -Pd bridging were observed for neutral and anionic Pd alkyl complexes, and in one case the aggregation mode was confirmed by X-ray diffraction.[15]

Generation of $[L_2Pd\{CH(CN)Et\}(PR_3)][B(C_6F_5)_4]$ Derivatives. To confirm the presence of a PdCH(CN)Et unit in **4a**−**e** and hence that 2,1 AN insertion occurs as proposed in Scheme 2, the reactions of **4a**−**e** with Lewis bases were explored. Complexes **4a**−**e** *do not* react with excess AN, CH_3CN or THF at 23 °C in CD_2Cl_2 solution. However, as shown in eq 3, **4a**−**e** react quantitatively with 1 equiv of PPh_3 (5 min, 23 °C) to yield $L_2Pd\{CH(CN)Et\}(PPh_3)^+$ cations **5a**−**e**, which have been characterized by multinuclear NMR and ESI−MS. Complex **5b** exists as two diastereomers due to the presence of two stereogenic centers. Complex **5c** also exists as two isomers, due to slow inversion of the chelate ring, which likely has a boat conformation similar to those in structurally characterized Pd^{II} complexes containing related bidentate N-donor ligands.[22] The ^1H NMR spectra of **5a**−**e** each contain a multiplet for the PdC*H*(CN)CH_2CH_3 methine hydrogen, which couples to the two methylene protons and phosphorus, multiplets for the diastereotopic PdCH(CN)C*H*$_2$$CH_3$ hydrogens, and a triplet for the PdCH(CN)CH_2C*H*$_3$ methyl group. The ^1H−^1H COSY spectra of **5a**−**e** show correlations between these resonances that are consistent with the PdCH(CN)CH_2CH_3 structure. The $^{13}C\{^1H\}$ NMR spectra of **5a**−**e** each contain a doublet (J_{CP} = 4−7 Hz) in the range δ 10−16 for PdCH(CN)Et methine carbon. The ^{31}P NMR spectra of **5a**−**e** each contain a PPh_3 resonance at ca. δ 35, which is shifted downfield from the free PPh_3 position (δ −5.0). The IR υ_{CN} bands for both **5a** and **5d** appear at 2192 cm^{-1}, ca. 56 cm^{-1} below the values for **4a**,**d**. These υ_{CN} values are similar to those for other complexes containing nonbridging MCR_2CN units,[9,11,23] such as (bipy)Pd$(CH_2CN)_2$ (2194 cm^{-1}),[21d] $(Me_2NCS_2)Pd(PEt_3)\{CH(CN)Me\}$ (2182 cm^{-1}),[9a] and [*cis*-Ir$(CO)_2(CH_2CN)_2]^-$ (2195 cm^{-1}).[24] The reduction in υ_{CN} on going from **4a**,**d** to **5a**,**d** is consistent with the change from bridging to terminal coordination of the PdCH(CN)Et unit.

The analogous PMe_3 adducts **6a**−**c** are formed in a similar manner (eq 3) and display similar spectroscopic properties.

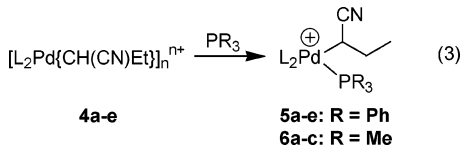

Attempts to isolate **5** or **6** using $B(C_6F_5)_4^-$ as the counterion were unsuccessful. However, **5d** was isolated as the $B\{3,5\text{-}(CF_3)_2\text{−}C_6H_3\}_4^-$ salt. The reaction of **4d′** with 1 equiv of PPh_3 in CH_2Cl_2 at 23 °C yields $[(Me_2bipy)Pd\{CH(CN)Et\}(PPh_3)][B\{3,5\text{-}(CF_3)_2\text{−}C_6H_3\}_4]$ (**5d′**) as an analytically pure yellow solid (74%). These results confirm the characterization of **4a**−**e** as 2,1 insertion products.

Generation of $[L_2Pd\{CH(CN)Et\}(CO)][B(C_6F_5)_4]$ (7a,b). As noted above, **4a**−**e** do not react with AN at 23 °C. This lack of reactivity arises because AN is not a sufficiently strong Lewis base to break up the PdCHEtCN- - -Pd bridging units in these aggregated cations. Similarly, **4a**−**e** do not react with ethylene at 23 °C (6 atm, 1 d; up to 25 atm for **4a**). No evidence for reaction of **4a** with ethylene (6 atm) was observed up to 50 °C, at which temperature Pd^0 formation was observed. To determine if insertions into Pd−CH(CN)R bonds are possible, the reactions of **4a**−**e** with the potentially more reactive substrate CO were explored.

Exposure of **4a**,**b** to 6 atm of CO at 23 °C results in rapid (5 min) formation of the CO adducts $L_2Pd\{CH(CN)Et\}(CO)^+$ (**7a**,**b**, eq 4). In contrast, **4c**−**e** do not react with CO under these conditions. **7b** exists as two diastereomers due to the presence of two stereogenic centers. The ^1H, ^{13}C, and COSY NMR spectra establish that **7a**,**b** each contain an α-cyano-propyl ligand. The Pd−*C*O ^{13}C NMR resonance appears at δ 174 for both **7a** and **7b**, close to the chemical shifts observed for the analogous acetyl carbonyl complexes (bim)Pd{C(═O)Me}-$(CO)^+$ (δ 173) and (Tbim)Pd{C(═O)Me}$(CO)^+$ (δ 172).[17] The IR υ_{CO} value for the terminal CO ligand of **7b** (2132 cm^{-1}) is higher than that of (Tbim)Pd{C(═O)Me}$(CO)^+$ (2118 cm^{-1}), which reflects the electron-withdrawing effect of the α-CN substituent.[17] For comparison, the υ_{CO} value for {(*n*hexyl)CH-(*N*-Me-imidazol-2-yl)$_2$}Pd$(CHCl_2)$(CO) is 2144 cm^{-1}.[25] The CO ligand of **7a** is labile, and decreasing the CO pressure to 1 atm or below results in the regeneration of **4a**. In contrast, **7b** is stable under 1 atm of CO for several hours.

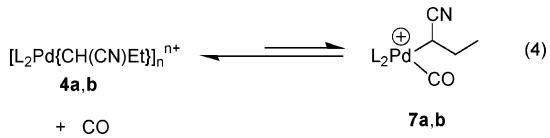

CO Insertion of (bim)Pd{CH(CN)Et}$(CO)^+$ (7a). Complex **7a** undergoes slow CO insertion (23 °C, 2 d) to yield an

(19) (a) Funabiki, T.; Hosomi, H.; Yoshida, S.; Tarama, K. *J. Am. Chem. Soc.* **1982**, *104*, 1560. (b) Odic, Y.; Pereyre, M. *J. Organomet. Chem.* **1973**, *55*, 273.

(20) Ruiz, J.; Rodríguez, V.; López, G.; Casabó, J.; Molins, E.; Miravitlles, C. *Organometallics* **1999**, *18*, 1177.

(21) For other examples see (a) Culkin, D. A.; Hartwig, J. F. *J. Am. Chem. Soc.* **2002**, *124*, 9330. (b) Naota, T.; Tannna, A.; Kamuro, S.; Murahashi, S. *J. Am. Chem. Soc.* **2002**, *124*, 6842. (c) Morvillo, A,; Bressan, M. *J. Organomet. Chem.* **1987**, *332*, 337. (d) Oehme, G.; Rober, K.; Pracejus, H. *J. Organomet. Chem.* **1976**, *105*, 127. (e) Falvello, L. R.; Fernandez, S.; Navarro, R.; Urriolabeitia, E. P. *Inorg. Chem.* **1997**, *36*, 1136.

(22) (a) Canty, A. J.; Minchin, N. J.; Skelton, B. W.; White, A. H. *Aust. J. Chem.* **1992**, *45*, 423. (b) Newkome, G. R.; Gupta, V. K.; Theriot, K. J.; Ewing, J. C.; Wicelinski, S. P.; Huie, W. R.; Fronczek, F. R.; Watkins, S. F. *Acta Crystallogr.* **1984**, *C40*, 1352. (c) Newkome, G. R.; Gupta, V. K.; Taylor, H. C. R.; Fronczek, F. R. *Organometallics* **1984**, *3*, 1549.

equilibrium mixture of **7a** and (bim)Pd{C(═O)CH(CN)Et}-$(CO)^+$ (**8a**, eq 5). The equilibrium constant for CO insertion, measured over a range of CO pressure (P_{CO}) of 4 to 20 atm, is $K_{eq} = [\mathbf{8a}][\mathbf{7a}]^{-1}P_{CO}^{-1} = 0.050(2)\ atm^{-1}$ at 23 °C. At 6 atm CO pressure, a ca. 1/3 mixture of **8a** and **7a** is formed, whereas at 20 atm of CO, a 1/1 mixture is formed. Complex **7b** does not insert CO under these conditions.

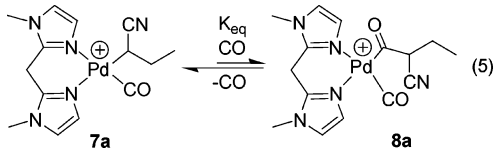

(5)

Complex **8a** has been characterized by multinuclear NMR. The Pd{*C*(═O)CH(CN)Et} acyl ^{13}C resonance appears at δ 213, close to the position observed for the acyl resonance in (bim)-Pd{*C*(═O)Me}$(CO)^+$ (δ 217).[17] The ^{13}C Pd{C(═O)*C*H(CN)-Et} methine resonance appears at δ 56.4, ca. 40 ppm downfield from the corresponding resonances of **5a**, **6a**, and **7a**, as expected due to the proximity of the carbonyl group.[26] The Pd-{C(═O)C*H*(CN)Et} methine ^1H resonance occurs at δ 3.51 (dd), ca. 1.7 ppm downfield from the corresponding resonances of **5a** and **6a**, and 0.7 ppm downfield from the corresponding resonance of **7a**. For comparison, the methine ^1H resonance for $CH_3C(═O)CH(CN)Et$ occurs at δ 3.70.[27] These assignments have been confirmed by experiments with ^{13}CO.[28]

Exposure of **8a** to vacuum results in regeneration of **4a**, confirming that the CO insertion of **7a** (eq 5) and the CO coordination of **4a** (eq 4) are reversible. For comparison, (bim)-Pd(Me)$(CO)^+$ inserts CO much more rapidly (<1 min at 23 °C, ca. 1 atm) than **7a** to yield (bim)Pd{C(═O)Me}$(CO)^+$ quantitatively and irreversibly.[17] Thus, the α-CN group clearly inhibits *but does not prevent* the CO insertion.

Generation of [(bim)Pd{CH(CNB(C_6F_5)$_3$)Et}(CH_2═CH_2)]-[B(C_6F_5)$_4$] (9a). As noted above, ethylene does not react with **4a**−**e** at 23 °C. One possible approach to promoting the reaction of $[L_2Pd\{CH(CN)Et\}]_n^{n+}$ species with olefins is to use a Lewis acid (A) to cleave the aggregates to form potentially more reactive monomeric $[L_2Pd\{CH(CN{-}A)Et\}^+$ species. The reaction of **4a** with B(C_6F_5)$_3$ and 10 equiv of ethylene (0 °C, 20 min) generates [(bim)Pd{CH(CNB(C_6F_5)$_3$)Et}(CH_2═CH_2)]-[B(C_6F_5)$_4$] (**9a**) quantitatively (eq 6). The ^{19}F NMR spectrum of **9a** contains a set of resonances at δ −134.9, −156.9, and −167.0 for the −CNB(C_6F_5)$_3$ unit, which are in the range observed for the nitrile adduct $CH_3CN{-}B(C_6F_5)_3$.[29] The ^1H and ^{13}C NMR spectra of **9a** contain resonances that are characteristic of an α-cyano-propyl group. The ethylene ^1H (δ 5.11) and ^{13}C (δ 94.1) resonances of **9a** both appear as broad singlets and are shifted upfield from the free ethylene positions (^1H: δ 5.38; ^{13}C: δ 123.0; at −60 °C). Exchange of free and **9a**-coordinated ethylene is slow on the NMR time scale at 0 °C, which contrasts with the fast ethylene exchange observed for (bim)Pd(Me)-$(CH_2$═$CH_2)^+$ at −60 °C.[17] Ethylene exchange of **9a**, which is expected to occur by an associative mechanism, is probably inhibited by the presence of the sterically bulky borane-capped α-cyano-propyl group. Complex **9a** decomposes to Pd^0 over several hours at 23 °C.

Scheme 3

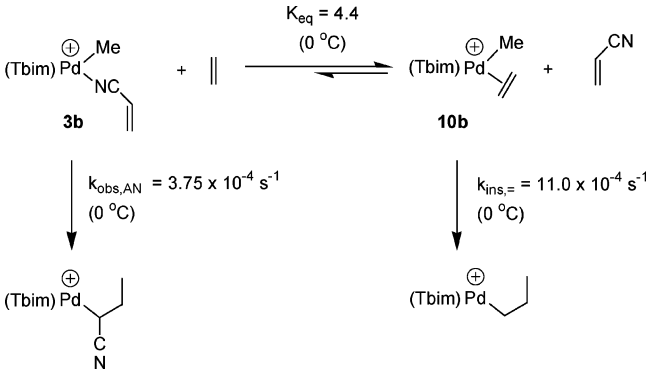

Complex **9a** does not undergo ethylene insertion at 23 °C. In contrast, (bim)Pd(Me)(CH_2═CH_2)$^+$ inserts ethylene rapidly above −10 °C.[17] Therefore, the presence of the electron-withdrawing α-CN−B(C_6F_5)$_3$ substituent clearly inhibits insertion of **9a**.

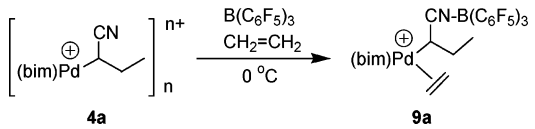

(6)

Comparative Ethylene and AN Coordination and Insertion. The relative binding strength and insertion kinetics of ethylene and AN were compared using the (Tbim)PdMe$^+$ system, as shown in Scheme 3. The equilibrium constant for the reaction of **3b** with ethylene to form **10b** and AN, K_{eq} = [**10b**][AN]/[**3b**][ethylene], was measured by ^1H NMR between −76 °C and −25 °C. Under these conditions, ethylene/AN exchange (i.e., **3b**/**10b** exchange) is slow on the NMR chemical shift time scale. At −25 °C, $K_{eq} = 6.3(1)$, and ethylene binding is favored over AN coordination. For example, at this temperature, the reaction of **3b** with 130 equiv of AN and 20 equiv of ethylene yields a ca. 1/1 equilibrium mixture of **3b** and **10b**. The reverse reaction, i.e., addition of excess AN to **10b** also affords an equilibrium mixture of **10b** and **3b**. A van't Hoff

(23) (a) Ittel, S. D.; Tolman, C. A.; English, A. D.; Jesson, J. P. *J. Am. Chem. Soc.* **1978**, *100*, 7577. (b) Ragaini, F.; Porta, F.; Fumagalli, A.; Demartin, F. *Organometallics* **1991**, *10*, 3785. (c) Ros, R.; Bataillard, R.; Roulet, R. *J. Organomet. Chem.* **1976**, *118*, C53. (d) Naota, T.; Tannna, A.; Murahashi, S.-I.; *J. Am. Chem. Soc.* **2000**, *122*, 2960.

(24) Porta, F.; Ragaini, F.; Cenini, S. *Organometallics* **1990**, *9*, 929.

(25) Foley, S. R.; Shen, H.; Qadeer, U. A.; Jordan, R. F. *Organometallics* **2004**, *23*, 600.

(26) The ^{13}C Pd{C(═O)*C*H(CN)Et} methine chemical shift of **8a** (δ 56.4) agrees reasonably well with the predicted value (δ 48.1) for $CH_3C(═O)CH(CN)$-Et, which is estimated using standard ^{13}C NMR chemical shift additivity rules. See Breitmaier, E.; Voelter, W. *Carbon-13 NMR*, 3rd ed.; VCH Publishers: Weinheim, Germany, 1987; pp 313−325.

(27) Itoh, T.; Fukuda, T.; Fujisawa, T. *Bull. Chem. Soc. Jpn.* **1989**, *62*, 3851.

(28) (a) The reaction of **4a** with ^{13}CO yields an equilibrium mixture of (bim)-Pd{CH(CN)Et}($^{13}CO)^+$ (**7a**-$^{13}C_1$) and (bim)Pd{^{13}C(═O)CH(CN)Et}($^{13}CO)^+$ (**8a**-$^{13}C_2$). The Pd{^{13}C(═O)C*H*(CN)Et} methine ^1H NMR resonance of **8a**-$^{13}C_2$ shows extra coupling not observed for **8a**, due to the labeled acyl carbonyl group. In addition, the Pd{^{13}C(═O)*C*H(CN)Et} methine ^{13}C NMR resonance of **8a**-$^{13}C_2$ is a doublet (δ 56.4, $^1J_{CC} = 25$). No $^2J_{CC}$ coupling is observed between the Pd{^{13}C(═O)CH(CN)Et} and Pd−^{13}CO carbons. (b) An unambiguous simulation of the Pd{^{13}C(═O)C*H*(CN)Et} methine ^1H NMR resonance of **8a**-$^{13}C_2$ to acquire $^2J_{CH}$ is not possible because the appearance of the simulated methine resonance is extremely sensitive to the assigned chemical shift values for the diastereotopic CH_2 hydrogens, which cannot be obtained due to overlapping of these resonances with the corresponding resonances of **7a**-$^{13}C_1$. This complication reflects the second-order character of the Pd{^{13}C(═O)C*H*(CN)CH_2CH_3} spin system, which results from the small chemical shift difference for the diastereotopic methylene hydrogens. However, if the chemical shifts of the methylene protons are taken as δ 1.92 and 1.91, the Pd{^{13}C(═O)C*H*(CN)Et} methine resonance is defined as ddd ($J_{HH} = 13.2$, 0.8; $^2J_{CH} = 6.6$). The $^2J_{CH}$ value determined in this way is consistent with a two-bond *C*(═O)C*H* coupling (cf. $^2J_{CH} = 5.5$ for acetone).

(29) Jacobsen, H.; Berke, H.; Döring, T.; Kehr, G.; Erker, G.; Fröhlich, R.; Meyer, O. *Organometallics* **1999**, *18*, 1724.

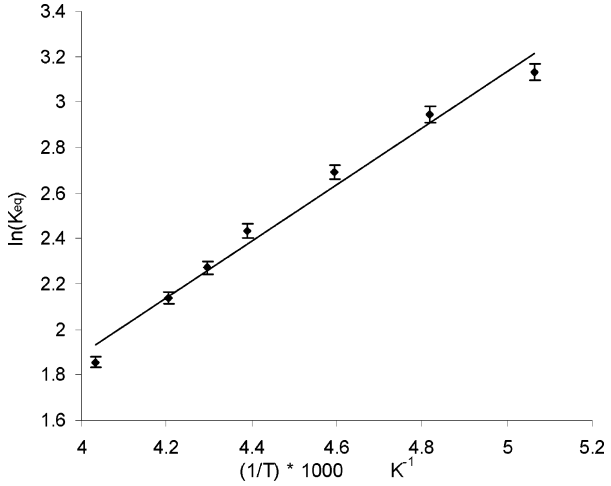

Figure 2. van't Hoff plot for the equilibrium in Scheme 3.

plot of the K_{eq} data (Figure 2) yields $\Delta H° = -2.5(1)$ kcal/mol, $\Delta S° = -6(1)$ eu for the equilibrium in Scheme 3. Using these thermodynamic parameters, K_{eq} is calculated to equal 4.4(3) at 0 °C.

The reaction of **3b** to produce **4b** is presumed to occur by reversible N/π-isomerization, followed irreversible migratory insertion and subsequent aggregation, as shown in Scheme 2. The observed first-order rate constant for conversion of **3b** to **4b** measured by the disappearance of the Pd−Me ^{1}H NMR resonance of **3b**, is $k_{obs,AN} = 3.75(3) \times 10^{-4}$ s^{-1} at 0 °C. Making the steady-state assumption for the unobserved π-complex intermediate, $k_{obs,AN} = k_1k_2/(k_{-1} + k_2)$ (see Scheme 2).[30] For comparison, the rate constant for ethylene insertion of **10b** is $k_{ins,=} = 11.0(2) \times 10^{-4}$ s^{-1} at 0 °C.[17]

These results show that AN coordinates more weakly and, overall, inserts more slowly than ethylene in the (Tbim)PdMe$^+$ system. Nevertheless, AN can compete with ethylene for insertion into (Tbim)PdMe$^+$. Assuming that AN/ethylene exchange (i.e., **3b**/**10b** exchange) is fast relative to insertion, the relative rates of formation of (Tbim)Pd{CH(CN)Et}$^+$ and (Tbim)PdPr$^+$ by reaction with AN and ethylene with (Tbim)PdMe$^+$ are given by eq 7.[31]

$$\frac{\text{rate of AN rxn}}{\text{rate ethylene rxn}} = \frac{(k_{obs,AN})[AN]}{K_{eq}(k_{ins,=})[\text{ethylene}]} \qquad (7)$$

For equal concentrations of AN and ethylene, this ratio is estimated to be 7/93 at 0 °C, based on the extrapolated K_{eq} value and measured values of $k_{obs,AN}$ and $k_{ins,=}$ at this temperature.

Discussion

The studies described above provide insights to the acrylonitrile (AN) coordination and insertion reactions of L$_2$PdR$^+$ olefin dimerization and polymerization catalysts, and the properties of the α-CN-alkyl metal species that result from AN insertion in these systems. The L$_2$PdMe$^+$ species **2a**−**f**, which contain a range of bidentate N-donor ligands (L$_2$) with different steric and electronic properties, coordinate AN to form N-bound L$_2$Pd(Me)(AN)$^+$ complexes **3a**-**f**. The C═C π-bound isomers were not detected. These observations are consistent with computational studies, which show that for the model system (HN═CHCH═NH)Pd(Et)(AN)$^+$, which is an analogue of **3f**, the N-bound form is ca. 13 kcal/mol more stable than the π-bound isomer.[32] The preference for N-coordination reflects the fact that the σ-donation component dominates the Pd-olefin bonding in L$_2$Pd(Me)(olefin)$^+$ species, due to the poor back-bonding ability of the cationic d^8 metal center, and the C═C bond of AN is a poor donor due to the low HOMO energy.

L$_2$PdMe(AN)$^+$ species **3a**−**e** undergo 2,1 AN insertion to yield L$_2$Pd{CH(CN)Et}$^+$ species. These reactions likely proceed by initial isomerization to the (unobserved) C═C π complexes followed by migratory insertion, and therefore the overall AN insertion rate will be determined by the energetics of the N/π isomerization and the insertion rate of the π complex. The strength of the Pd−N interaction and hence the stability of the N-bound adducts should be enhanced as the net positive charge on the metal center is increased. The overall insertion rates are slower for the pyridine and diimine AN complexes **3c**−**f** than for the bim and Tbim complexes **3a**,**b**, which is opposite to the trend in insertion rates of the corresponding ethylene complexes.[7,17] IR ν_{CO} data for the terminal carbonyl ligands in L$_2$Pd{C═O)Me}(CO)$^+$ species (Figure 1) show that the metal centers in the pyridine and diimine complexes are electron-poor relative to those in the bim and Tbim complexes. Therefore, the slower AN insertion rates of **3c**−**f** can be ascribed to stronger N-coordination of AN in these species. Steric crowding in **3f** may also disfavor the π complex and thereby contribute to the absence of insertion in this case. It is interesting to note in this context that calculated gas-phase barriers for insertion of the model π complexes (HN═CHCH═NH)Pd(R)(AN)$^+$ and (HN═CHCH═NH)Pd(R)(ethylene)$^+$ differ by only ca. 1−2 kcal/mol.[32,33]

The AN insertions of **3a**−**e** occur with 2,1 regioselectivity; i.e., Michael-type addition is observed. This regioselectivity is consistent with computational results that show 2,1 insertion is favored by ca. 5 kcal/mol for (HN═CHCH═NH)Pd(R)(AN)$^+$ model species.[32,33] The Cp_z coefficient in the AN LUMO is larger at the terminal carbon (C1) than the internal carbon (C2), which favors migration of the alkyl to C1, and the M−CHRCN bond is expected to be stronger than the M−CH$_2$CHRCN bond that would be formed by 1,2 insertion.

ESI−MS and NMR studies show that L$_2$Pd{CH(CN)Et}$^+$ species derived from AN insertion of **3a**−**e** form robust [L$_2$Pd{CH(CN)Et}]$_n^{n+}$ aggregates (**4a**−**e**). The structures of these aggregates could not be determined, but IR data and literature precedents strongly suggest that the monomer units are linked by PdCHRCN- - -Pd bridges. These interactions are strong because the PdCHR*CN* group is more electron-rich and hence

(30) The N/π-isomerization could occur intramolecularly as shown in Scheme 2 or by an associative mechanism involving free AN. However, the $k_{obs,AN}$ value for **3b** is essentially the same in the absence of free AN (i.e., when **3b** is generated from **2b** using a deficiency of AN) and in the presence of 140 equiv of free AN, so possible associative N/π isomerization does not influence the overall rate of insertion.

(31) As AN/ethylene exchange occurs by associative ligand substitution, the rate will depend on the concentrations of free ethylene and AN. EXSY studies show that the first-order rate constants for conversion of **3b** to **10b** (1.8×10^{-2} s^{-1}) and **10b** to **3b** (2.9×10^{-3} s^{-1}) at −30 °C with [ethylene] = 0.26 M and [AN] = 1.4 M are much larger than the $k_{obs,AN}$ and $k_{ins,=}$ values determined at 0 °C. Thus, under typical conditions, AN/ethylene exchange will be fast relative to insertion for the Tbim system.

(32) (a) Philipp, D. M.; Muller, R. P.; Goddard, W. A., III; Storer, J.; McAdon, M.; Mullins, M. *J. Am. Chem. Soc.* **2002**, *124*, 10198. (b) Deubel, D. K.; Ziegler, T. *Organometallics* **2002**, *21*, 1603.

(33) (a) Deubel, D. K.; Ziegler, T. *Organometallics* **2002**, *21*, 4432. (b) von Schenck, H.; Strömberg, S.; Zetterberg, K.; Ludwig, M.; Åkermark, B.; Svensson, M. *Organometallics* **2001**, *20*, 2813.

more Lewis basic than a conventional nitrile, due to the presence of the metal at C_α. The PdCHRCN- - -Pd bridging is sufficiently strong that neither AN nor ethylene break up the aggregates to form $L_2Pd\{CH(CN)Et\}(monomer)^+$ complexes, and therefore additional insertion reactions leading to polymerization or copolymerization are not observed. In contrast, the binding affinities of acetonitrile and ethylene to $(phen)PdMe^+$ are nearly equal,[34] and $L_2Pd(R)(NCMe)^+$ species are effective catalysts for ethylene polymerization, and ethylene/acrylate and olefin/CO copolymerizations.[7c,35] Complexes **4a**−**e** do react with phosphines to form $L_2Pd\{CH(CN)Et\}(PR_3)^+$ complexes (**5a**−**e** and **6a**−**c**), which enabled definitive characterization of the 2,1 insertion regiochemistry. Complex **4a** reacts with ethylene in the presence of $B(C_6F_5)_3$ to form $(bim)Pd\{CH(CNB(C_6F_5)_3)Et\}(CH_2{=}CH_2)^+$ (**9a**), but this species is resistant to insertion due to the poor nucleophilicity and steric bulk of the borane-capped cyanoalkyl group.

The two most electron-rich $[L_2Pd\{CH(CN)Et\}]_n^{n+}$ species among those studied, **4a**,**b**, react with CO to form $L_2Pd\{CH(CN)Et\}(CO)^+$ complexes **7a**,**b**, whereas **4c**−**e** do not. The reactivity of $[L_2Pd\{CH(CN)Et\}]_n^{n+}$ with CO is determined by the lability of PdCHEtCN- - -Pd bridges and the ability of the $L_2Pd\{CH(CN)Et\}^+$ unit to stabilize the coordinated CO by back-bonding, both of which are enhanced by the strong donor imidazole ligands of **4a**,**b**. In the presence of excess CO, **7a** undergoes reversible CO insertion to form $(bim)Pd\{C(=O)CH(CN)Et\}(CO)^+$ (**8a**), whereas **7b** does not. The CO insertion of **7a** is disfavored both kinetically and thermodynamically relative to CO insertion of the corresponding methyl complex $(bim)Pd(Me)(CO)^+$. These results are consistent with previous studies of CO insertion into M−R bonds, which have shown that electron-withdrawing substituents on the migrating R group generally inhibit migration and destabilize the insertion product, while electron-releasing substituents have the opposite effects.[36] This trend has been ascribed to differences in bond strengths ($M-R^{EWG} > M-R$) and differences in the basicity/nucleophilicity of the migrating group ($R > R^{EWG}$). It is also possible that steric crowding inhibits insertion of **7a** and especially **7b**. Nevertheless, the observation that **7a** reversibly inserts CO suggests that insertion reactions of suitably designed $L_2M\{CH(CN)R\}$(olefin) species may also be possible.

Studies of ligand exchange equilibria and insertion kinetics of $(Tbim)Pd(Me)(AN)^+$ (**3b**) and $(Tbim)Pd(Me)(ethylene)^+$ (**10b**) show that AN coordinates more weakly and, overall, inserts more slowly than ethylene in the $(Tbim)Pd(Me)^+$ system. The slower insertion of **3b** vs **10b** reflects the requirement for N/π isomerization of **3b**. Nevertheless, the differences in monomer binding and insertion rates are sufficiently small that AN insertion should be competitive with ethylene insertion in this and related systems.

Conclusions

The reactions of acrylonitrile (AN) with representative L_2PdMe^+ olefin dimerization and polymerization catalysts that contain bidentate N-donor ligands (L_2) have been studied to probe the possibility of polymerizing this substrate by insertion polymerization. L_2PdMe^+ species form N-bound $L_2Pd(Me)(AN)^+$ adducts that undergo 2,1 AN insertion to yield $L_2Pd\{CH(CN)Et\}^+$ products. These insertions likely proceed via intermediate C=C π complexes, which, however, were not detected. The ability of the N-bound isomers to isomerize to the π complexes is critical for insertion, and highly electron-deficient, sterically crowded L_nMR^+ species for which the N-bound adduct is strongly favored over the π-complex, such as **3f**, are poor candidates for AN insertion. The $L_2Pd\{CH(CN)Et\}^+$ insertion products form robust aggregates by PdCHEtCN- - -Pd bridging, due to the enhanced Lewis basicity of the α-metalated nitrile group. The $[L_2Pd\{CH(CN)Et\}]_n^{n+}$ aggregate species studied here are not readily cleaved by ethylene or AN, and therefore do not undergo further insertions of these substrates. However, it should be possible to prevent aggregation of this type by steric blocking using suitably designed ligands or by site-isolation of active catalyst species on a support. The bis-imidazole species $(bim)Pd\{CH(CN)Et\}(CO)^+$ (**7a**) undergoes reversible CO insertion to form $(bim)Pd\{C(=O)CH(CN)Et\}(CO)^+$ (**8a**), but this process is disfavored both kinetically and thermodynamically relative to CO insertion of $(bim)Pd(Me)(CO)^+$, due to the electron-withdrawing effect of the α-CN substituent. The low insertion reactivity of α-CN-substituted $L_nMCHRCN$ species is the key obstacle to insertion polymerization and copolymerization of AN.

Experimental Section

General Procedures. All manipulations were performed under purified N_2 or vacuum using standard Schlenk or high vacuum techniques or in a nitrogen-filled drybox unless otherwise noted. Nitrogen was purified by passage through columns of activated molecular sieves and Q-5 oxygen scavenger. Chlorinated solvents were distilled from CaH_2, and acrylonitrile (AN) was distilled from $CaCl_2$, and these materials were stored under vacuum prior to use. PMe_3 was purchased from Aldrich and dried over 4 Å molecular sieves. PPh_3, CO, ^{13}CO and ethylene were purchased from Aldrich and used as received. $[HNMe_2Ph][B(C_6F_5)_4]$, $[Li(Et_2O)_{2.8}][B(C_6F_5)_4]$, $Na[B(3,5\text{-}C_6H_3(CF_3)_2)_4]$, and $B(C_6F_5)_3$ were obtained from Boulder Scientific and used as received. Compounds **1a**,[37] **1b**,**c**,[17] **1d**,**e** and **2d**,**e**,[18] and **1f**[7e] were prepared by literature procedures.

NMR spectra were recorded in sealed tubes on a Bruker AMX-500 spectrometer at ambient temperature unless otherwise indicated. ^1H and ^{13}C chemical shifts are reported versus Me_4Si and were determined by reference to the residual solvent peaks. ^{19}F and ^{31}P chemical shifts were referenced to external neat $CFCl_3$ and H_3PO_4, respectively. Coupling constants are reported in Hz. NMR spectra of $B(C_6F_5)_4^-$ salts contain anion resonances at the free anion positions.[38] NMR spectra of **3a**−**c** and species derived from these species contain resonances for free

(34) Rix, F. C.; Brookhart, M.; White, P. S. *J. Am. Chem. Soc.* **1996**, *118*, 4746.
(35) (a) Mecking, S.; Johnson, L. K.; Wang, L.; Brookhart, M. *J. Am. Chem. Soc.* **1998**, *120*, 888. (b) Brookhart, M.; Rix, F. C.; DeSimone, J. M.; Barborak, J. C. *J. Am. Chem. Soc.* **1992**, *114*, 5894. (c) Done, M. C.; Ruther, T.; Cavell, K. J.; Kilner, M.; Peacock, E. J.; Braussaud, N.; Skelton, B. W.; White, A. *J. Organomet. Chem.* **2002**, *607*, 78.
(36) (a) Axe, F. U.; Marynick, D. S. *J. Am. Chem. Soc.* **1988**, *110*, 3728. (b) Cotton, J. D.; Markwell, R. D. *J. Organomet. Chem.* **1990**, *388*, 123. (c) Cotton, J. D.; Crisp, G. T.; Daly, V. A. *Inorg. Chim. Acta* **1981**, *47*, 165. (d) Cross, R. J.; Gemmill, J. *J. Chem. Soc., Dalton Trans.* **1981**, 2317. (e) Cawse, J. N.; Fiato, R. A.; Pruett, R. L. *J. Organomet. Chem.* **1979**, *172*, 405. (f) Anderson, G. K.; Cross, R. J. *Acc. Chem. Res.* **1984**, *17*, 67. (g) Kuhlmann, E. J.; Alexander, J. J. *Coord. Chem. Rev.* **1980**, *33*, 195. (h) Calderazzo, F.; Noack, K. *Coord. Chem. Rev.* **1966**, *1*, 118. (i) Koga, N.; Morokuma, K. *J. Am. Chem. Soc.* **1986**, *108*, 6136. (j) Ros, R.; Renaud, J.; Roulet, R. *J. Organomet. Chem.* **1974**, *77*, C4.
(37) Byers, P. K.; Canty, A. J. *Organometallics* **1990**, *9*, 210.
(38) NMR data for free $B(C_6F_5)_4^-$: $^{13}C\{^1H\}$ NMR (CD_2Cl_2): δ 148.5 (dm, J = 234, C2), 138.6 (dm, J = 246, C4), 136.6 (dm, J = 243, C3), 123.6 (br, C1). ^{19}F NMR (CD_2Cl_2): δ −133.2 (br s, 2F, *o*-F), −163.7 (t, J = 23, 1F, *p*-F), −167.6 (t, J = 19, 2F, *m*-F). $^{13}C\{^1H\}$ NMR (CD_2Cl_2, −60 °C): δ 147.5 (dm, J = 241, C2), 137.8 (dm, J = 238, C4), 135.8 (dm, J = 249, C3), 123.6 (br, C1). ^{19}F NMR (CD_2Cl_2, −60 °C): δ −133.7 (br s, 2F, *o*-F), −163.0 (t, J = 23, 1F, *p*-F), −167.0 (t, J = 19, 2F, *m*-F).

NMe_2Ph.[39] Samples of CD_2Cl_2 solutions of **2d**−**f** and species generated in situ from **2d-f** contain LiCl. NMR spectra for species generated in the presence of excess AN contain resonances for free AN.[40,41]

ESI-MS experiments were performed with a HP Series 1100MSD instrument using direct injection via a syringe pump (ca. 10^{-6} M solutions). Good agreement between observed and calculated isotope patterns was observed in all cases. In each case, the listed *m*/*z* value corresponds to the most intense peak in the isotope pattern. Infrared spectra were recorded on a Nicolet NEXUS 470 FT-IR spectrometer. Unless otherwise noted, IR spectra were recorded for neat samples using the Nicolet Smart Miracle ATR accessory after the evaporation of the solvent.

The following procedure was used to quantity the CO in the carbonylation reactions. A valved NMR tube containing the reaction solution was attached to a vacuum line, the solution was frozen with liquid nitrogen, the tube was evacuated, and the valve was closed. The vacuum line was isolated from the pumping system and charged with CO. The NMR tube valve was opened to allow CO into the tube and then was closed. The amount of CO that was added to the tube was determined from the decrease in CO pressure in the vacuum line.

[(bim)PdMe(NMe$_2$Ph)][B(C$_6$F$_5$)$_4$] (2a). An NMR tube was charged with (bim)$PdMe_2$ (**1a**, 4.0 mg, 0.013 mmol) and $[HNMe_2Ph][B(C_6F_5)_4]$ (10.0 mg, 0.013 mmol), and CD_2Cl_2 (0.6 mL) was added by vacuum transfer at −78 °C. The tube was vigorously agitated resulting in a pale yellow solution. The tube was maintained at −78 °C for 10 min and then transferred to the NMR probe at −60 °C. NMR spectra showed that **2a** had formed quantitatively. ^{1}H NMR (CD_2Cl_2, −60 °C): δ 7.85 (d, J = 8, 2H, *o*-Ph), 7.44 (t, J = 8, 2H, *m*-Ph), 7.30 (t, J = 7, 1H, *p*-Ph), 6.89 (s, 1H, imidazole), 6.88 (s, 1H, imidazole), 6.59 (s, 1H, imidazole), 4.98 (s, 1H, imidazole), 4.13 (s, 2H, CH_2), 3.66 (s, 3H, imidazole N*Me*), 3.58 (s, 3H, imidazole N*Me*), 2.92 (s, 6H, N*Me*$_2$Ph), 0.76 (s, 3H, PdMe). ^{13}C{^{1}H} NMR (CD_2Cl_2, −60 °C): δ 152.9 (Ph C1), 141.8 (imidazole C2), 140.7 (imidazole C2), 129.1 (Ph C2), 127.5 (Ph C4), 126.9 (imidazole C4), 125.6 (imidazole C4), 121.9 (Ph C3), 121.5 (imidazole C5), 121.4 (imidazole C5), 52.9 (N*Me*$_2$Ph), 34.3 (imidazole N*Me*), 33.7 (imidazole N*Me*), 22.5 (CH_2), 2.1 (PdMe).[42]

[(Tbim)PdMe(NMe$_2$Ph)][B(C$_6$F$_5$)$_4$] (2b). This complex was generated quantitatively from (Tbim)$PdMe_2$ (**1b**, 11.0 mg, 0.018 mmol) and $[HNMe_2Ph][B(C_6F_5)_4]$ (14.7 mg, 0.018 mmol) using the procedure for **2a**. ^{1}H NMR (CD_2Cl_2, −60 °C): δ 7.84 (d, J = 8, 2H, *ortho* NMe$_2$*Ph*), 7.41 (t, J = 8, 2H, *meta*-NMe$_2$*Ph*), 7.28 (t, J = 7, 1H, *para*-NMe$_2$*Ph*), 7.01 (d, J = 7, 6H, tolyl H2), 6.86 (s, 1H, imidazole), 6.80 (s, 1H, imidazole), 6.60 (br s, 6H, tolyl H3), 6.50 (s, 1H, imidazole), 5.57 (s, 1H, CH), 5.24 (s, 1H, imidazole), 3.15 (s, 3H, imidazole N*Me*), 2.89 (s, 3H, imidazole N*Me*), 2.84 (s, 3H, N*Me*$_2$Ph), 2.54 (s, 3H, N*Me*$_2$Ph), 2.30 (s, 9H, tolyl Me), 0.30 (s, 3H, PdMe). ^{13}C{^{1}H} NMR (CD_2Cl_2, −60 °C): δ 152.9 (C1 of NMe$_2$*Ph*), 143.1 (imidazole C2), 143.0 (imidazole C2), 137.5 (tolyl C_{ipso}), 137.4 (tolyl C_{ipso}), 131.3 (br s, tolyl C3), 129.2 (C2 of NMe$_2$*Ph*), 128.3 (imidazole C4), 128.0 (br s, tolyl C2), 127.0 (C4 of NMe$_2$*Ph*), 125.0 (imidazole C4), 122.3 (imidazole C5), 122.2 (C3 of NMe$_2$*Ph*), 121.9 (imidazole C5), 64.4 ((tolyl)$_3$*C*), 56.0 (N*Me*$_2$Ph), 50.4 (N*Me*$_2$Ph), 45.0 (CH), 36.1 (imidazole N*Me*), 33.7 (imidazole N*Me*), 20.5 (tolyl Me), 4.5 (PdMe).

[(CH$_2$py′$_2$)PdMe(NMe$_2$Ph)][B(C$_6$F$_5$)$_4$] (2c). This complex was generated quantitatively from (CH_2py′$_2$)$PdMe_2$ (**1c**, 5.6 mg, 0.017 mmol) and $[HNMe_2Ph][B(C_6F_5)_4]$ (13.4 mg, 0.017 mmol) using the procedure for **2a**. Inversion of the chelate ring is slow on the NMR time scale at −60 °C. ^{1}H NMR (CD_2Cl_2, −60 °C): δ 8.20 (s, 1H, py′ H6), 7.63 (d, J = 8, 2H, *o*-Ph), 7.56 (d, J = 8, 1H, py′ H4), 7.45 (t, J = 8, 2H, *m*-Ph), 7.39 (d, J = 8, 1H, py′ H4), 7.31 (m, 2H, *p*-Ph and py′ H3), 7.22 (d, J = 8, 1H, py′ H3), 5.97 (s, 1H, py′ H6), 5.08 (d, J = 13.8, 1H, CH_2), 4.22 (d, J = 13.8, 1H, CH_2), 2.95 (s, 3H, N*Me*$_2$Ph), 2.90 (s, 3H, N*Me*$_2$Ph), 2.27 (s, 3H, py′ Me), 1.86 (s, 3H, py′ Me), 0.91 (s, 3H, PdMe). ^{13}C{^{1}H} NMR (CD_2Cl_2, −60 °C): δ 153.7 (py′ C2), 152.5 (Ph C1), 151.8 (py′ C2), 151.3 (py′ C6), 149.4 (py′ C6), 139.7 (py′ C4), 139.2 (py′ C4), 134.2 (py′ C5), 133.1 (py′ C5), 129.2 (Ph C2), 126.9 (Ph C4), 124.2 (py′ C3), 124.0 (py′ C3), 121.6 (Ph C3), 54.7 (N*Me*$_2$Ph), 49.7 (N*Me*$_2$Ph), 46.5 (CH_2), 17.8 (py′ Me), 17.7 (py′ Me), 5.4 (PdMe).

[{(2,6-^{i}Pr$_2$-diimine)PdMe}$_2$(μ-Cl)][B(C$_6$F$_5$)$_4$] (2f).[7d] An NMR tube was charged with (2,6-^{i}Pr$_2$-diimine)PdMeCl (**1f**, 12.4 mg, 0.029 mmol) and $[Li(Et_2O)_{2.8}][B(C_6F_5)_4]$ (26.3 mg, 0.029 mmol), and CD_2Cl_2 (0.6 mL) was added by vacuum transfer at −196 °C. The tube was warmed to 23 °C resulting in slurry of a white solid in a an orange supernatant. After 10 min, NMR spectra showed that **2f** had formed quantitatively. ^{1}H NMR (CD_2Cl_2): δ 7.34 (t, J = 8, 2H, Ar H4), 7.26 (d, J = 7, 4H, Ar H3), 7.17 (t, J = 8, 2H, Ar H4), 7.09 (d, J = 8, 4H, Ar H3), 2.89 (septet, J = 6, 4H, C*H*Me$_2$), 2.75 (septet, J = 6, 4H, C*H*Me$_2$), 2.05 (s, 6H, N=C*Me*), 2.00 (s, 6H, N=C*Me*), 1.22 (d, J = 7, 12H, CH*Me*$_2$), 1.12 (d, J = 7, 12H, CH*Me*$_2$), 1.07 (d, J = 7, 12H, CH*Me*$_2$), and 1.00 (d, J = 7, 12H, CH*Me*$_2$), 0.41 (s, 6H, PdMe).

[(bim)PdMe(NCCH=CH$_2$)][B(C$_6$F$_5$)$_4$] (3a). An NMR tube containing a solution of [(bim)PdMe(NMe$_2$Ph)][B(C$_6$F$_5$)$_4$] (**2a**, 0.013 mmol) in CD_2Cl_2 (0.6 mL) was cooled to −196 °C and acrylonitrile (0.195 mmol) was added by vacuum transfer. The tube was warmed to −78 °C and vigorously agitated resulting in a pale yellow solution. The tube was maintained at −78 °C for 10 min and then transferred to the NMR probe at −60 °C. A ^{1}H NMR spectrum showed that [(bim)PdMe(NCCH=CH$_2$)][B(C$_6$F$_5$)$_4$] (**3a**) had formed quantitatively. Separate sharp ^{1}H NMR resonances for free and coordinated AN were observed at −60 and 23 °C. ^{1}H NMR (CD_2Cl_2, −60 °C): δ 6.99 (d, J = 1, 1H, imidazole), 6.97 (d, J = 1, 1H, imidazole), 6.92 (d, J = 1, 1H, imidazole), 6.86 (d, J = 1, 1H, imidazole), 6.55 (d, J = 18, 1H, H_{trans} of coordinated AN), 6.43 (d, J = 12, 1H, H_{cis} of coordinated AN), 5.93 (dd, J = 18, 12, 1H, H_{int} of coordinated AN), 4.08 (s, 2H, CH_2), 3.71 (s, 3H, N*Me*), 3.68 (s, 3H, N*Me*), 0.75 (s, 3H, PdMe). ^{13}C{^{1}H} NMR (CD_2Cl_2, −60 °C): δ 143.0 (C_{ter} of coordinated AN), 140.1 (imidazole C2), 139.0 (imidazole C2), 126.1 (imidazole C4), 125.6 (imidazole C4), 122.1 (imidazole C5), 121.8 (imidazole C5), 119.2 (*C*N of coordinated AN), 105.7 (C_{int} of coordinated AN), 34.6 (N*Me*), 33.7 (N*Me*), 22.7 (CH_2), −2.7 (PdMe). The ^{13}C NMR assignments for the coordinated AN were confirmed by a DEPT-135 experiment. IR (neat): υ_{CN} = 2244 cm^{-1}.

[(Tbim)PdMe(NCCH=CH$_2$)][B(C$_6$F$_5$)$_4$] (3b). A solution of [(Tbim)PdMe(NMe$_2$Ph)][B(C$_6$F$_5$)$_4$] (**2b**, 0.018 mmol) in CD_2Cl_2 (0.6 mL) was generated in an NMR tube, and AN (0.162 mmol) was added by vacuum transfer at −196 °C. The tube was maintained at −30 °C for 30 min to achieve complete displacement of NMe$_2$Ph by AN. A ^{1}H NMR spectrum was obtained at −60 °C and showed that **3b** had formed quantitatively. Separate sharp resonances for free and coordinated AN were observed at −60 and 0 °C. ^{1}H NMR (CD_2Cl_2, −60 °C): δ 6.99 (d, J = 8, 6H, tolyl H2), 6.83 (d, J = 1, 1H, imidazole), 6.82 (d, J = 1, 1H, imidazole), 6.81 (d, J = 1, 1H, imidazole), 6.77 (d, J = 1, 1H, imidazole), 6.51 (d, J = 18, 1H, H_{trans} of coordinated AN), 6.50 (br d, J = 8, 6H, tolyl H3), 6.44 (d, J = 12, 1H, H_{cis} of coordinated AN),

(39) (a) NMR data for free NMe$_2$Ph: ^{1}H NMR (CD_2Cl_2): δ 7.20 (m, 2H, *o*-Ph), 6.72 (m, 2H, *m*-Ph), 6.67 (t, J = 7, 1H, *p*-Ph), 3.03 (s, 6H, Me). ^{13}C{^{1}H} NMR (CD_2Cl_2): δ 151.1 (C1), 129.3 (C2), 116.6 (C4), 112.8 (C3), 40.7 (Me). ^{1}H NMR (CD_2Cl_2, −60 °C): δ 7.18 (m, 2H, *o*-Ph), 6.67 (m, 2H, *m*-Ph), 6.63 (t, J = 7, 1H, *p*-Ph), 2.88 (s, 6H, Me). ^{13}C{^{1}H} NMR (CD_2Cl_2, −60 °C): δ 150.2 (C1), 128.7 (C2), 115.8 (C4), 111.9 (C3), 40.3 (Me). (b) If excess $[HNMe_2Ph][B(C_6F_5)_4]$ is used in the generation of **3a**−**c**, the excess $HNMe_2Ph^+$ undergoes fast H^+ exchange with NMe$_2$Ph and a single set of NMe$_2$Ph/$HNMe_2Ph^+$ resonances at the weighted average of the chemical shifts of these species is observed.

(40) NMR data for free AN: ^{1}H NMR (CD_2Cl_2, 23 °C): δ 6.21 (d, J = 18, 1H, H_{trans}), 6.07 (d, J = 12, 1H, H_{cis}), 5.67 (dd, J = 18, 12.0, 1H, H_{int}). ^{13}C{^{1}H} NMR (CD_2Cl_2): δ 138.0 (C_{ter}), 117.3 (*C*N), 108.2 (C_{int}). ^{1}H NMR (CD_2Cl_2, −60 °C): δ 6.24 (d, J = 18, 1H, H_{trans}), 6.09 (d, J = 12, 1H, H_{cis}), 5.69 (dd, J = 18, 12.0, 1H, H_{int}). ^{13}C{^{1}H} NMR (CD_2Cl_2, −60 °C): δ 138.1 (C_{ter}), 117.3 (*C*N), 107.2 (C_{int}).

(41) ^{13}C NMR assignments for AN from Schumann, H.; Speis, M.; Bosman, W. P.; Smits, J. M. M.; Beurskens, P. T. *J. Organomet. Chem.* **1991**, *403*, 165.

(42) Assignments of the imidazole C4 and C5 resonances are based on data in Katritzky, A. R.; Pozharskii, A. F. *Handbook of Heterocyclic Chemistry*, 2nd ed.; Pergamon Publisher: New York, 2000; pp 108−112.

5.90 (dd, J = 18, 12, 1H, H_{int} of coordinated AN), 5.65 (s, 1H, CH), 3.15 (s, 3H, N*Me*), 3.05 (s, 3H, N*Me*), 2.27 (s, 9H, tolyl Me), 0.33 (s, 3H, PdMe). $^{13}C\{^1H\}$ NMR (CD_2Cl_2, −60 °C): δ 143.4 (imidazole C2), 142.5 (C_{ter} of coordinated AN), 141.2 (imidazole C2), 137.6 (tolyl C_{ipso}), 137.3 (tolyl C_{ipso}), 131.4 (tolyl C3), 127.8 (tolyl C2),126.6 (imidazole C4), 125.7 (imidazole C4), 123.0 (imidazole C5), 121.9 (imidazole C5), 118.0 (*C*N of coordinated AN), 105.7 (C_{int} of coordinated AN), 65.1 ((tolyl)$_3$*C*), 44.6 (CH), 35.3 (N*Me*), 34.5 (N*Me*), 20.5 (tolyl Me), −4.0 (PdMe).

[(CH$_2$py′$_2$)PdMe(NCCH═CH$_2$)][B(C$_6$F$_5$)$_4$] (3c). This complex was generated quantitatively in CD_2Cl_2 solution from [(CH$_2$py′$_2$)PdMe(NMe$_2$-Ph)][B(C$_6$F$_5$)$_4$] (**2c**, 0.017 mmol) and AN (0.527 mmol) using the procedure for **3a**. The ^1H NMR spectrum contains separate sharp resonances for free and coordinated AN at −60 °C and separate but broad resonances for free and coordinated AN at 23 °C. ^1H NMR (CD_2Cl_2, −60 °C): δ 8.22 (s, 1H, py′ H6), 8.17 (s, 1H, py′ H6), 7.66 (d, J = 8, 1H, py′ H4), 7.63 (d, J = 8, 1H, py′ H4), 7.40 (d, J = 8, 1H, py′ H3), 7.38 (d, J = 8, 1H, py′ H3), 6.55 (d, J = 18, 1H, H_{trans} of coordinated AN), 6.45 (d, J = 12, 1H, H_{cis} of coordinated AN), 5.94 (dd, J = 18, 12, 1H, H_{int} of coordinated AN), 4.72 (d, J = 14.2, 1H, CH_2), 4.20 (d, J = 14.2, 1H, CH_2), 2.30 (s, 3H, py′ Me), 2.29 (s, 3H, py′ Me), 0.88 (s, 3H, PdMe). $^{13}C\{^1H\}$ NMR (CD_2Cl_2, −60 °C): δ 153.2 (py′ C2), 151.9 (py′ C6), 150.7 (py′ C2), 149.6 (py′ C6), 143.7 (C_{ter} of coordinated AN), 140.6 (py′ C4), 140.2 (py′ C4), 134.8 (py′ C5), 134.3 (py′ C5), 125.1 (py′ C3), 124.6 (py′ C3), 119.7 (*C*N of coordinated AN), 105.8 (C_{int} of coordinated AN), 45.8 (CH_2), 18.0 (py′ Me), 17.9 (py′ Me), 0.9 (PdMe).

[(Me$_2$bipy)PdMe(NCCH═CH$_2$)][B(C$_6$F$_5$)$_4$] (3d). A solution of [{-(Me$_2$bipy)PdMe}$_2$(μ-Cl)][B(C$_6$F$_5$)$_4$] (**2d**, 0.0075 mmol) and 0.5 equiv [Li(Et$_2$O)$_{2.8}$][B(C$_6$F$_5$)$_4$] (0.0075 mmol) in CD_2Cl_2 (0.6 mL) was generated in an NMR tube, and AN (0.45 mmol) was added by vacuum transfer at −196 °C. The tube was warmed to 23 °C, resulting in immediate formation of a slurry of a white solid in a pale yellow supernatant. ^1H NMR spectra showed that **3d** had formed in >95% yield. The ^1H NMR spectrum contains separate sharp resonances for free and coordinated AN at −60 °C and separate but broad resonances for free and coordinated AN at 23 °C. ^1H NMR (CD_2Cl_2, −60 °C): δ 8.29 (d, J = 7, 1H, bipy H6), 8.28 (d, J = 6, 1H, bipy H6), 7.96 (s, 1H, bipy H3), 7.94 (s, 1H, bipy H3), 7.41 (d, J = 6, 1H, bipy H5), 7.40 (d, J = 7, 1H, bipy H5), 6.66 (d, J = 18, H_{trans} of coordinated AN), 6.52 (d, J = 12, H_{cis} of coordinated AN), 6.03 (dd, J = 18, 12, H_{int} of coordinated AN), 2.51 (s, 3H, bipy Me), 2.49 (s, 3H, bipy Me), 0.94 (s, 3H, PdMe). $^{13}C\{^1H\}$ NMR (CD_2Cl_2, −60 °C): δ 156.3 (bipy C2), 153.1 (bipy C4), 152.5 (bipy C4), 151.8 (bipy C2), 147.9 (bipy C6), 147.4 (bipy, C6), 143.8 (C_{ter} of coordinated AN), 127.8 (bipy), 127.4 (bipy), 123.8 (bipy), 122.9 (bipy), 120.4 (*C*N of coordinated AN), 105.5 (C_{int} of coordinated AN), 21.4 (bipy Me), 21.3 (bipy Me), 2.8 (PdMe). ESI−MS: [(Me$_2$bipy)PdMe(NCCH═CH$_2$)]$^+$ calcd. *m*/*z* 358.1, found 358.0. IR (neat): υ_{CN} = 2247 cm^{-1}.

[(t Bu$_2$bipy)PdMe(NCCH═CH$_2$)][B(C$_6$F$_5$)$_4$] (3e). This complex was generated quantitatively in CD_2Cl_2 (0.6 mL) from **2e** (0.014 mmol) in the presence of [Li(Et$_2$O)$_{2.8}$][B(C$_6$F$_5$)$_4$] (0.014 mmol) and AN (0.39 mmol) using the procedure for **3d**. The ^1H NMR spectrum contains separate but broad resonances for free and coordinated AN at 23 °C. ^1H NMR (CD_2Cl_2): δ 8.43 (d, J = 6, 1H, bipy H6), 8.35 (d, J = 6, 1H, bipy H6), 8.12 (d, J = 2, 1H, bipy H3), 8.11 (d, J = 2, 1H, bipy H3), 7.61 (dd, J = 6, 2, 1H, bipy H5), 7.60 (dd, J = 6, 2, 1H, bipy H5**)**, 6.66 (br d, J = 18, 1H, H_{trans} coordinated AN), 6.53 (d, J = 12, 1H, H_{cis} of coordinated AN), 1.43 (s, 9H, CMe_3), 1.42 (s, 9H, CMe_3), 1.06 (s, 3H, PdMe); the H_{int} resonance for coordinated AN was not observed due to exchange broadening and/or interference from the free AN resonances. $^{13}C\{^1H\}$ NMR (CD_2Cl_2): δ 165.7 (bipy C2), 165.3 (bipy C2), 157.1 (bipy C4), 152.6 (bipy C4), 148.5 (bipy C6), 147.8 (bipy, C6), 124.4 (bipy), 124.0 (bipy), 120.1 (bipy), 119.1 (bipy), 35.6 (*C*Me$_3$), 35.6 (*C*Me$_3$), 29.8 (C*Me*$_3$), 29.7 (C*Me*$_3$), 2.9 (PdMe); resonances for coordinated AN were not observed due to exchange broadening.

[(2,6-^{i}Pr$_2$-diimine)Pd(Me)(NCCH═CH$_2$)][B(C$_6$F$_5$)$_4$] (3f). This complex was generated quantitatively in CD_2Cl_2 (0.6 mL) from **2f** (0.014 mmol) in the presence of [Li(Et$_2$O)$_{2.8}$][B(C$_6$F$_5$)$_4$] (0.014 mmol) and AN (0.18 mmol) using the procedure for **3d**. The NMR spectra contain separate sharp resonances for free and coordinated AN at 23 °C. ^1H NMR (CD_2Cl_2): δ 7.34 (m, 6H, Ar), 6.19 (d, J = 12, 1H, H_{cis} of coordinated AN), 5.81 (d, J = 18, 1H, H_{trans} of coordinated AN), 5.44 (dd, J = 18, 12, 1H, H_{int} of coordinated AN), 2.95 (septet, J = 7, 2H, C*H*Me$_2$), 2.89 (septet, J = 7, 2H, C*H*Me$_2$),2.24 (s, 3H, N═C*Me*), 2.23 (s, 3H, N═C*Me*), 1.37 (d, J = 7, 6H, CH*Me*$_2$), 1.34 (d, J = 7, 6H, CH*Me*$_2$), 1.24 (d, J = 7, 6H, CH*Me*$_2$), 1.20 (d, J = 7, 6H, CH*Me*$_2$), 0.55 (s, 3H, PdMe). $^{13}C\{^1H\}$ NMR (CD_2Cl_2): δ 180.3 (N═*C*), 172.7 (N═*C*), 144.3 (C_{ter} of coordinated AN), 140.7 (Ar C1), 140.6 (Ar C1), 138.6 (Ar C2), 138.0 (Ar C2), 129.3 (Ar C4),128.6 (Ar C4), 124.9 (Ar C3), 124.6 (Ar C3), 120.5 (*C*N of coordinated AN), 104.5 (C_{int} of coordinated AN), 29.5 (*C*HMe$_2$), 29.3 (*C*HMe$_2$), 23.8 (CH*Me*$_2$), 23.7 (CH*Me*$_2$), 23.4 (CH*Me*$_2$), 23.0 (CH*Me*$_2$), 21.8 (N═C*Me*), 20.1 (N═C*Me*), 7.4 (PdMe). ESI−MS: [(2,6-^{i}Pr$_2$-diimine)PdMe(NCCH═CH$_2$)]$^+$ calcd. *m*/*z* 578.2, found 578.2.

[(bim)Pd{CH(CN)CH$_2$CH$_3$}]$_n^{n+}$ (B(C$_6$F$_5$)$_4^-$ salt, 4a). An NMR tube containing a solution of [(bim)PdMe(NCCH═CH$_2$)][B(C$_6$F$_5$)$_4$] (**3a**, 0.013 mmol) and AN (0.182 mmol) in CD_2Cl_2 (0.6 mL) was maintained at 23 °C and monitored periodically by ^1H NMR. The NMR signals of **3a** disappeared after 10 h. The volatiles were removed under vacuum to yield a pale yellow solid. The solid was dissolved in CD_2Cl_2 (0.6 mL). NMR and ESI−MS analyses showed that [(bim)Pd{CH(CN)-CH$_2$CH$_3$}]$_n^{n+}$ (**4a**) had formed quantitatively. ^1H NMR (CD_2Cl_2) Major resonances: δ 7.10 (d, J = 1, 1H, imidazole), 7.05 (d, J = 1, 1H, imidazole), 7.03 (d, J = 1, 1H, imidazole), 7.02 (d, J = 1, 1H, imidazole), 6.99 (d, J = 1, 1H, imidazole), 6.93 (d, J = 1, 1H, imidazole), 6.91 (d, J = 1, 1H, imidazole), 6.87 (d, J = 1, 1H, imidazole), 6.86 (d, J = 1, 1H, imidazole), 6.83 (br s, 2H, imidazole), 6.82 (d, J = 1, 1H, imidazole), 4.14 (s, 2H, CH_2), 4.12 (s, 2H, CH_2), 4.09 (s, 2H, CH_2), 3.78 (s, 3H, N*Me*), 3.76 (s, 3H, N*Me*), 3.75 (s, 3H, N*Me*), 3.74 (s, 3H, N*Me*), 3.69 (s, 3H, N*Me*), 3.68 (s, 3H, N*Me*), 2.49 (br m, 3H, PdC*H*(CN)), 2.22 (m, 1H, PdCH(CN)C*H*$_2$), 2.13 (m, 1H, PdCH(CN)C*H*$_2$), 2.05 (m, 2H, PdCH(CN)C*H*$_2$), 1.90 (m, 1H, PdCH-(CN)C*H*$_2$), 1.78 (m, 1H, PdCH(CN)C*H*$_2$), 1.25−1.10 (m, 9H, PdCH(CN)CH$_2$C*H*$_3$). Major cations observed in ESI-MS: (bim)Pd-{CH(CN)CH$_2$CH$_3$}]$^+$ calcd. *m*/*z* 350.1, found 350.1; [(bim)Pd{CH(CN)-CH$_2$CH$_3$}]$_2^{2+}$ calcd. *m*/*z* 350.1, found 350.1; {[(bim)Pd{CH(CN)CH$_2$-CH$_3$}]$_3^{3+}$[B(C$_6$F$_5$)$_4$]$^-$} calcd. *m*/*z* 865.5, found 865.2. IR (neat): υ_{CN} = 2246 cm^{-1}.

[(Tbim)Pd{CH(CN)CH$_2$CH$_3$}]$_n^{n+}$ (B(C$_6$F$_5$)$_4^-$ salt, 4b). This species was generated quantitatively from **3b** (0.018 mmol) and AN (0.144 mmol) in 40 min at 23 °C using the procedure for **4a**. The observed first-order rate constant for conversion of **3b** to **4b**, determined from the disappearance of the PdMe ^1H NMR resonance, is k_{obs}(23 °C) = 2.06(4) × 10^{-3} s^{-1} at 23 °C ([AN] = 2.6 M, 70 equiv excess vs **3b**), k_{obs}(0 °C) = 3.75(3) × 10^{-4} s^{-1} at 0 °C ([AN] = 0.82 M, 20 equiv excess vs **3b**), k_{obs}(0 °C) = 4.03(5) × 10^{-4} s^{-1} at 0 °C ([AN] = 1.6 M, 140 equiv excess vs **3b**), and k_{obs}(0 °C) = 4.5(2) × 10^{-4} s^{-1} at 0 °C (no free AN; **3b** generated from **2b** and 0.7 equiv AN). ^1H NMR (CD_2Cl_2) Major resonances: δ 7.14−7.10 (m, 6H, tolyl H2), 7.00−6.76 (m, 4H, imidazole H), 6.63−6.46 (m, 6H, tolyl H3), 5.90−5.72 (m, 1H, CH), 3.57−3.00 (m, 6H, imidazole N*Me*), 2.40−2.20 (m, 9H, tolyl Me), 2.17−1.70 (m, 1H, PdC*H*(CN)), 1.53−0.81 (m, 5H, PdCH(CN)-C*H*$_2$ and PdCH(CN)CH$_2$C*H*$_3$). Key cations observed in ESI−MS: (Tbim)Pd{CH(CN)CH$_2$CH$_3$}]$^+$ calcd. *m*/*z* 634.2, found 634.1; {[(Tbim)-Pd{CH(CN)CH$_2$CH$_3$}]$_2^{2+}$-(*p*-tolyl)$_3$C$^+$} calcd. *m*/*z* 983.3, found 983.1.

[(CH$_2$py′$_2$)Pd{CH(CN)CH$_2$CH$_3$}]$_n^{n+}$ (B(C$_6$F$_5$)$_4^-$ salt, 4c). This species was generated quantitatively from **3c** (0.017 mmol) and AN (0.510 mmol) in 2 d at 23 °C using the procedure for **4a**. ^1H NMR

(CD_2Cl_2) Major resonances: δ 8.45−7.30 (m, 6H, py′), 4.90−4.60 (m, 1H, CH_2), 4.50−4.20 (m, 1H, CH_2), 2.50−2.20 (m, 6H, py′ Me), 2.20−2.05 (m, 1H, PdC*H*(CN)), 2.00−1.40 (m, 2H, PdCH(CN)CH_2), 1.40−0.90 (m, 3H, PdCH(CN)CH_2CH_3). Major cations observed in ESI−MS: $(CH_2py'_2)Pd\{CH(CN)CH_2CH_3\}^+$ calcd. *m*/*z* 372.1, found 371.9; $[(CH_2py'_2)Pd\{CH(CN)CH_2CH_3\}]_2^{2+}$ calcd. *m*/*z* 372.1, found 371.9; $\{[(CH_2py'_2)Pd\{CH(CN)CH_2CH_3\}]_3^{3+}[B(C_6F_5)_4]^-\}$ calcd. *m*/*z* 897.6, found 897.8.

$[(Me_2bipy)Pd\{CH(CN)CH_2CH_3\}]_n^{n+}$ $(B(C_6F_5)_4^-$ salt, 4d). This species was generated quantitatively from **3d** (0.015 mmol) and AN (0.430 mmol) in 2 d at 23 °C using the procedure for **4a**. ^{1}H NMR (CD_2Cl_2) Major resonances: δ 8.46−7.90 (m, 4H, bipy), 7.56−7.34 (m, 2H, bipy), 2.76−2.47 (m, 7H, PdC*H*(CN) and bipy Me), 2.17−1.64 (m, 2H, PdCH(CN)CH_2), 1.44−1.11 (m, 3H, PdCH(CN)CH_2CH_3). Major cation observed in ESI−MS: $(Me_2bipy)Pd\{CH(CN)CH_2CH_3\}^+$ calcd. *m*/*z* 358.1, found 358.0. IR (neat): ν_{CN} = 2249 cm^{-1}.

$[(Me_2bipy)Pd\{CH(CN)CH_2CH_3\}]_n^{n+}$ $(B(3,5\text{-}C_6H_3(CF_3)_2)_4^-$ salt, 4d′). A flask was charged with (Me_2bipy)PdMeCl (**1d**, 100 mg, 0.29 mmol) and Na[B(3,5-$C_6H_3(CF_3)_2)_4$] (260 mg, 0.29 mmol), and CH_2Cl_2 (40 mL) was added at −78 °C by vacuum transfer. The pale yellow slurry was vigorously stirred for 5 min at 23 °C. The flask was cooled to −196 °C and AN (0.2 mL, 3.0 mmol) was added by vacuum transfer. The flask was warmed to 23 °C and the mixture was stirred for 2 d to yield a slurry of a white solid in a yellow supernatant. The mixture was filtered through diatomaceous earth and the yellow filtrate was dried under vacuum to afford a yellow solid (290 mg, 81%). Anal. Calcd for $C_{48}H_{30}BF_{24}N_3Pd$: C, 47.18; H, 2.47; N, 3.44. Found: C, 47.35; H, 2.65; N, 3.38. The NMR data for **4d′** are very similar to the data for **4d**, with the exception of the anion resonances.[43]

$[(^tBu_2bipy)Pd\{CH(CN)CH_2CH_3\}]_n^{n+}$ $(B(C_6F_5)_4^-$ salt, 4e). This species was generated quantitatively from **3e** (0.028 mmol) and AN (0.36 mmol) after 38 h at 23 °C using the procedure for **4a**. ^{1}H NMR (CD_2Cl_2) Major resonances: δ 8.50−7.96 (m, 4H, bipy), 7.73−7.56 (m, 2H, bipy), 2.75−2.52 (m, 1H, PdC*H*(CN)), 2.22−1.64 (m, 2H, PdCH(CN)CH_2), 1.50−1.11 (m, 21H, CMe_3 and PdCH(CN)CH_2CH_3). Major cation observed in ESI−MS: $(^tBu_2bipy)Pd\{CH(CN)CH_2CH_3\}^+$ calcd. *m*/*z* 442.1, found 442.0.

$[(bim)Pd\{CH(CN)CH_2CH_3\}(PPh_3)][B(C_6F_5)_4]$ (5a). Solid PPh_3 (3.3 mg, 0.013 mmol) was added to an NMR tube containing solid $[(bim)Pd\{CH(CN)CH_2CH_3\}]_n^{n+}$ ($B(C_6F_5)_4^-$ salt, **4a**, 0.013 mmol). The tube was evacuated and CD_2Cl_2 (0.6 mL) was added by vacuum transfer at −78 °C. The tube was vigorously agitated to yield an off-white solution and was then warmed to 23 °C. After 5 min, NMR spectra showed that $(bim)Pd\{CH(CN)CH_2CH_3\}(PPh_3)^+$ (**5a**) had formed in 90% yield. ^{1}H NMR (CD_2Cl_2): δ 7.68 (m, 7H, *o*-Ph and imidazole), 7.57 (m, 3H, *p*-Ph), 7.48 (m, 6H, *m*-Ph), 7.02 (m, 1H, imidazole), 6.40 (d, J = 2, 1H, imidazole), 5.71 (d, J = 2, 1H, imidazole), 4.26 (d, J = 17, 1H, CH_2), 4.22 (d, J = 17, 1H, CH_2), 3.78 (s, 3H, N*Me*), 3.62 (s, 3H, N*Me*), 1.72 (ddd, J_{HH} = 12.9, 8.5; J_{HP} = 6.9, 1H, PdC*H*(CN)CH_2), 1.30 (m, 2H, PdCH(CN)CH_2), 0.67 (t, J = 7, 3H, PdCH(CN)CH_2CH_3). ^{13}C{^{1}H} NMR (CD_2Cl_2): δ 141.6 (imidazole C2), 141.0 (imidazole C2), 134.6 (d, J = 11, *o*-Ph), 132.4 (d, J = 3, *p*-Ph), 129.6 (d, J = 10, *m*-Ph), 128.2 (d, J = 52, Ph C_{ipso}), 128.0 (imidazole C4), 127.3 (imidazole C4), 123.8 (*C*N), 122.6 (d, J = 2, imidazole C5), 122.0 (imidazole C5), 34.6 (N*Me*), 34.3 (N*Me*), 25.5 (PdCH(CN)*C*H_2), 23.2 (CH_2), 15.2 (PdCH(CN)CH_2*C*H_3), 13.2 (d, J = 4, Pd*C*H(CN)CH_2). ^{31}P{^{1}H} NMR (CD_2Cl_2): δ 35.1 (s, PPh_3). Key ^{1}H-^{1}H COSY correlations δ/δ: 1.72 (PdC*H*(CN)CH_2)/1.30 (PdCH(CN)CH_2); 1.30 (PdCH(CN)-CH_2)/0.67 (PdCH(CN)CH_2*C*H_3). ESI−MS: (bim)Pd{CH(CN)CH_2-CH_3}$(PPh_3)^+$ calcd. *m*/*z* 612.1, found 612.0. $B(C_6F_5)_4^-$ calcd. *m*/*z* 679.0, found 678.7. IR (neat): ν_{CN} = 2192 cm^{-1}.

$[(Tbim)Pd\{CH(CN)CH_2CH_3\}(PPh_3)][B(C_6F_5)_4]$ (5b). This compound was generated in 90% yield from **4b** (0.018 mmol) and PPh_3 (6.7 mg, 0.025 mmol) using the procedure for **5a**. **5b** exists as two diastereomers. The diastereomer ratio was 3/1 after 5 min and reached a constant value of 1/1 after 24 h at 23 °C. *NMR data for major diastereomer:* ^{1}H NMR (CD_2Cl_2): δ 7.60 (m, 6H, PPh_3), 7.46 (m, 4H, PPh_3 and imidazole), 7.35 (m, 6H, PPh_3), 7.12 (d, J = 8, 6H, tolyl H2), 6.94 (s, 1H, imidazole), 6.83 (d, J = 8, 6H, tolyl H3), 6.28 (d, J = 1, 1H, imidazole), 5.97 (s, 1H, imidazole), 5.35 (s, 1H, CH), 3.25 (s, 3H, N*Me*), 2.68 (s, 3H, N*Me*), 2.37 (s, 9H, tolyl Me), 1.70 (m, 1H, PdC*H*(CN)CH_2), 1.20 (m, 2H, PdCH(CN)CH_2), 0.79 (t, J = 8, 3H, PdCH(CN)CH_2*C*H_3). ^{13}C{^{1}H} NMR (CD_2Cl_2): δ 144.9 (imidazole C2), 144.2 (imidazole C2), 139.3 (tolyl C_{ipso}), 138.6 (tolyl C_{ipso}), 134.8 (d, J = 11, *o*-Ph), 132.4 (tolyl C3), 132.3 (d, J = 4, *p*-Ph), 129.7 (d, J = 11, *m*-Ph), 129.4 (imidazole C), 129.1 (tolyl C2), 128.2 (imidazole C), 127.7 (d, J = 27, PPh_3 C_{ipso}), 125.9 (*C*N), 123.5 (d, J = 3, imidazole C), 121.6 (imidazole C), 66.0 ((tolyl)$_3$*C*), 45.6 (CH), 36.8 (N*Me*), 33.7 (N*Me*), 25.6 (br s, PdCH(CN)*C*H_2), 21.0 (tolyl Me), 15.3 (PdCH(CN)-CH_2*C*H_3), 13.5 (br s, Pd*C*H(CN)CH_2). ^{31}P{^{1}H} NMR (CD_2Cl_2): δ 34.0 (s, PPh_3). Key ^{1}H−^{1}H COSY correlations δ/δ: 1.70 (PdC*H*(CN)CH_2)/1.20 (PdCH(CN)CH_2); 1.20 (PdCH(CN)CH_2)/0.79 (PdCH(CN)CH_2*C*H_3). Key ^{1}H-^{13}C HMQC correlations δ ^{1}H/δ ^{13}C: 1.70 (PdC*H*(CN))/13.5 (Pd*C*H(CN)); 1.20 (PdCH(CN)CH_2)/25.6 (PdCH(CN)*C*H_2); 0.79 (PdCH-(CN)CH_2CH_3)/15.3 (PdCH(CN)CH_2*C*H_3). *NMR data for minor diastereomer:* ^{1}H NMR (CD_2Cl_2): δ 7.80 (s, 1H, imidazole), 7.56 (m, 6H, PPh_3), 7.51 (m, 3H, PPh_3), 7.29 (m, 6H, PPh_3), 7.05 (d, J = 8, 6H, tolyl H2), 6.92 (s, 1H, imidazole), 6.64 (d, J = 8, 6H, tolyl H3), 6.39 (d, J = 1.4, 1H, imidazole), 5.89 (s, 1H, imidazole), 5.73 (s, 1H, CH), 3.17 (s, 3H, N*Me*), 3.00 (s, 3H, N*Me*), 2.31 (s, 9H, tolyl Me), 1.70 (m, 1H, PdC*H*(CN)CH_2), 1.60 (m, 2H, PdCH(CN)CH_2), 0.73 (t, J = 8, 3H, PdCH(CN)CH_2CH_3). ^{13}C{^{1}H} NMR (CD_2Cl_2): δ 144.6 (imidazole C2), 144.4 (imidazole C2), 139.7 (tolyl C_{ipso}), 138.4 (tolyl C_{ipso}), 134.8 (d, J = 11, *o*-Ph), 132.2 (d, J = 4, *p*-Ph), 132.0 (tolyl C3), 129.6 (d, J = 11, *m*-Ph), 129.2 (imidazole C), 129.0 (tolyl C2), 128.4 (imidazole C), 128.1 (d, J = 40, PPh_3 C_{ipso}), 125.8 (*C*N), 123.4 (d, J = 3, imidazole C), 122.0 (imidazole C), 65.8 ((tolyl)$_3$*C*), 46.1 (CH), 36.2 (N*Me*), 34.9 (N*Me*), 25.8 (PdCH(CN)*C*H_2), 20.9 (tolyl Me), 15.0 (PdCH(CN)-CH_2*C*H_3), 11.9 (d, J = 7, Pd*C*H(CN)CH_2). ^{31}P{^{1}H} NMR (CD_2Cl_2): δ 33.4 (s, PPh_3). Key ^{1}H−^{1}H COSY correlations δ/δ: 1.70 (PdC*H*(CN)-CH_2)/1.60 (PdCH(CN)CH_2); 1.60 (PdCH(CN)CH_2)/0.73 (PdCH(CN)-CH_2CH_3). Key ^{1}H−^{13}C HMQC correlations δ ^{1}H/δ ^{13}C: 1.70 (PdC*H*-(CN))/11.9 (Pd*C*H(CN)); 1.60 (PdCH(CN)CH_2)/25.8 (PdCH(CN)*C*H_2); 0.73 (PdCH(CN)CH_2CH_3)/15.0 (PdCH(CN)CH_2*C*H_3). ESI−MS: (Tbim)-$Pd\{CH(CN)CH_2CH_3\}(PPh_3)^+$ calcd. *m*/*z* 896.2, found 896.2. $B(C_6F_5)_4^-$ calcd. *m*/*z* 679.0, found 678.7.

$[(CH_2py'_2)Pd\{CH(CN)CH_2CH_3\}(PPh_3)][B(C_6F_5)_4]$ (5c). This compound was generated quantitatively from **4c** (0.016 mmol) and PPh_3 (4.2 mg, 0.016 mmol) using the procedure for **5a**. **5c** exists as two diastereomers. The diastereomer ratio was 5/1 after 5 min and did not change after 24 h at 23 °C. *NMR data for major diastereomer:* ^{1}H NMR (CD_2Cl_2): δ 9.12 (s, 1H, py′ H6), 7.75 (d, J_{HP} = 8, 1H, py′ H6), 7.61 (m, 8H, *o*-Ph and py′ H4), 7.48 (m, 6H, *m*-Ph), 7.35 (m, 5H, *p*-Ph and py′ H3), 5.00 (d, J = 14, 1H, CH_2), 4.37 (d, J = 14, 1H, CH_2), 2.42 (s, 3H, py′ Me), 1.81 (ddd, J_{HH} = 12.1, 10.7; J_{HP} = 4.6, 1H, PdC*H*(CN)CH_2), 1.74 (s, 3H, py′ Me), 1.33 (m, 1H, PdCH(CN)CH_2), 1.02 (m, 1H, PdCH(CN)CH_2), 0.65 (t, J = 7, 3H, PdCH(CN)CH_2CH_3). ^{13}C{^{1}H} NMR (CD_2Cl_2): δ 151.8 (py′ C2), 151.7 (d, J = 2, py′ C6), 151.6 (py′ C2), 149.7 (py′ C6), 141.1 (py′ C4), 140.1 (py′ C4), 135.1 (d, J = 2, py′ C5), 134.4 (py′ C5), 133.9 (d, J = 11, *o*-Ph), 132.1 (d, J = 3, *p*-Ph), 129.3 (d, J = 11, *m*-Ph), 126.8 (d, J = 53, Ph C_{ipso}), 125.6 (*C*N), 125.1 (d, J = 2, py′ C3), 124.3 (py′ C3), 45.8 (CH_2), 25.9 (PdCH(CN)*C*H_2), 17.9 (py′ Me), 17.7 (py′ Me), 14.6 (PdCH(CN)-CH_2CH_3), 12.1 (d, J = 5, Pd*C*H(CN)CH_2). ^{31}P{^{1}H} NMR (CD_2Cl_2): δ 34.0 (s, PPh_3). Key ^{1}H-^{1}H COSY correlations δ/δ: 1.81 (PdC*H*(CN)-CH_2)/1.33 (PdCH(CN)CH_2); 1.81 (PdC*H*(CN)CH_2)/1.02 (PdCH(CN)-CH_2); 1.33 (PdC*H*(CN)CH_2)/1.02 (PdCH(CN)CH_2); 1.33 (PdCH(CN)-

(43) NMR spectra of $B\{3,5\text{-}C_6H_3(CF_3)_2\}_4^-$ salts contain resonances at the free anion positions. ^{1}H NMR (CD_2Cl_2): δ 7.72 (s, 8H, H2), 7.55 (s, 4H, H4). ^{13}C{^{1}H} NMR (CD_2Cl_2): δ 162.1 (q, J_{CB} = 234, C1), 135.1 (C2), 129.2 (q, J_{CF} = 32, C3), 125.0 (q, J_{CF} = 273, CF_3), 117.8 (m, C4). ^{19}F NMR (CD_2Cl_2): δ −62.8 (s). ^{11}B NMR (CD_2Cl_2): δ −6.7 (s).

CH_2)/0.65 (PdCH(CN)CH$_2$CH_3); 1.02 (PdCH(CN)CH_2)/0.65 (PdCH(CN)-CH$_2$CH_3). *NMR data for minor diastereomer:* ^{1}H NMR (CD_2Cl_2): δ 8.51 (s, 1H, py′ H6), 7.66−7.21 (m, 20H, PPh_3 and py′ H), 5.19 (d, J = 13, 1H, CH_2), 4.44 (d, J = 13, 1H, CH_2), 2.39 (s, 3H, py′ Me), 1.81 (m, 1H, PdCH(CN)CH$_2$), 1.74 (s, 3H, py′ Me), 1.02 (m, 2H, PdCH-(CN)CH_2), 0.55 (t, J = 7, 3H, PdCH(CN)CH$_2$CH_3). ^{13}C{^{1}H} NMR (CD_2Cl_2): δ 151.5 (py′ C6), 150.3 (py′ C6), 141.0 (py′ C4), 140.0 (py′ C4), 133.8 (d, J = 11, *o*-Ph), 132.1 (d, J = 3, *p*-Ph), 129.3 (d, J = 11, *m*-Ph), 126.6 (d, J = 53, Ph C_{ipso}), 125.4 (*C*N), 124.8 (d, J = 2, py′ C3), 124.3 (py′ C3), 46.4 (CH_2), 22.9 (PdCH(CN)*C*H$_2$), 17.9 (py′ Me), 17.7 (py′ Me), 14.5 (PdCH(CN)CH$_2$*C*H$_3$), 10.3 (d, J = 5, Pd*C*H-(CN)CH$_2$). The py′ C2 and C5 resonances were not observed. ^{31}P{^{1}H} NMR (CD_2Cl_2): δ 34.2 (s, PPh_3). ESI-MS: (CH$_2$py′$_2$)Pd{CH(CN)CH$_2$-CH$_3$}(PPh$_3$)$^+$ calcd. *m*/*z* 634.2, found 633.9. B(C$_6$F$_5$)$_4^-$ calcd. *m*/*z* 679.0, found 678.7.

[(Me$_2$bipy)Pd{CH(CN)CH$_2$CH$_3$}(PPh$_3$)][B(C$_6$F$_5$)$_4$] (5d). This compound was generated in 85% yield in 4 h at 23 °C from **4d** (0.015 mmol) and PPh_3 (3.8 mg, 0.015 mmol) using the procedure for **5a**. ^{1}H NMR (CD_2Cl_2): δ 8.99 (br, 1H, bipy H6), 8.04 (s, 1H, bipy H3), 7.95 (s, 1H, bipy H3), 7.80 (m, 6H, *o*-Ph), 7.62 (m, 4H, *p*-Ph and bipy H5), 7.52 (m, 6H, *m*-Ph), 7.26 (d, J = 6, 1H, bipy H6), 6.75 (d, J = 6, 1H, bipy H5), 2.61 (s, 3H, bipy Me), 2.39 (s, 3H, bipy Me), 1.99 (ddd, J_{HH} = 12.5, 6.3; J_{HP} = 10.2, 1H, PdCH(CN)CH$_2$), 1.64 (m, 1H, PdCH-(CN)CH_2), 1.40 (m, 1H, PdCH(CN)CH_2), 0.74 (t, J = 7, 3H, PdCH-(CN)CH$_2$CH_3). ^{13}C{^{1}H} NMR (CD_2Cl_2): δ 155.9 (bipy C2), 155.4 (bipy C2), 154.6 (bipy C4), 153.8 (bipy C4), 151.0 (bipy C6), 149.8 (bipy, C6), 135.1 (d, J = 11, *o*-Ph), 133.0 (d, J = 2, *p*-Ph), 129.9 (d, J = 11, *m*-Ph), 128.5 (bipy), 127.6 (d, J = 53, PPh_3 C_{ipso}), 127.5 (bipy), 125.7 (*C*N), 124.1 (bipy), 124.0 (bipy), 24.5 (PdCH(CN)*C*H$_2$), 21.7 (bipy Me), 21.5 (bipy Me), 15.7 (d, J = 6, Pd*C*H(CN)CH$_2$), 15.0 (PdCH-(CN)CH$_2$*C*H$_3$). ^{31}P{^{1}H} NMR (CD_2Cl_2): δ 38.7 (s, PPh_3). Key ^{1}H−^{1}H COSY correlations δ/δ: 1.99 (PdCH(CN)CH$_2$)/1.64 (PdCH(CN)-CH_2); 1.99 (PdCH(CN)CH$_2$)/1.40 (PdCH(CN)CH_2); 1.64 (PdCH(CN)-CH_2)/1.40 (PdCH(CN)CH_2); 1.64 (PdCH(CN)CH_2)/0.74 (PdCH(CN)-CH$_2$CH_3); 1.40 (PdCH(CN)CH_2)/0.74 (PdCH(CN)CH$_2$CH_3). ESI-MS: (Me$_2$bipy)Pd{CH(CN)CH$_2$CH$_3$}(PPh$_3$)$^+$ calcd. *m*/*z* 620.1, found 620.0. IR (neat): ν_{CN} = 2196 cm^{-1}.

[(Me$_2$bipy)Pd{CH(CN)CH$_2$CH$_3$}(PPh$_3$)][B(3,5-C$_6$H$_3$(CF$_3$)$_2$)$_4$] (5d′). A flask was charged with (Me$_2$bipy)PdMeCl (**1d**, 100 mg, 0.29 mmol) and Na[B(3,5-C$_6$H$_3$(CF$_3$)$_2$)$_4$] (260 mg, 0.29 mmol), and CH_2Cl_2 (40 mL) was added at −78 °C by vacuum transfer. The pale yellow slurry was vigorously stirred for 5 min at 23 °C. The flask was cooled to −196 °C and AN (0.2 mL, 3.0 mmol) was added by vacuum transfer. The flask was warmed to 23 °C and the mixture was stirred for 2 d to yield a slurry of a white solid in a pale yellow supernatant. A solution of PPh_3 (75 mg, 0.29 mmol) in CH_2Cl_2 (5 mL) was added by syringe. The mixture was stirred for 6 h at 23 °C to afford a white slurry in yellow supernatant. The mixture was filtered through diatomaceous earth and the yellow filtrate was dried under vacuum to afford a yellow solid (320 mg, 74%). Anal. Calcd for $C_{66}H_{45}BF_{24}N_3PPd$: C, 53.41; H, 3.06; N, 2.83. Found: C, 53.57; H, 3.39; N, 2.85. The NMR data for **5d′** are identical with the data for **5d** with the exception of the anion resonances.[43]

[(*t*Bu$_2$bipy)Pd{CH(CN)CH$_2$CH$_3$}(PPh$_3$)][B(C$_6$F$_5$)$_4$] (5e). This compound was generated in 90% yield in 1 h at 23 °C from **4e** (0.026 mmol) and PPh_3 (6.7 mg, 0.026 mmol) using the procedure for **5a**. ^{1}H NMR (CD_2Cl_2): δ 9.09 (br, 1H, bipy H6), 8.17 (s, 1H, bipy H3), 8.09 (s, 1H, bipy H3), 7.81 (m, 7H, *o*-Ph and bipy H5), 7.63 (m, 3H, *p*-Ph), 7.53 (m, 6H, *m*-Ph), 7.34 (br, 1H, bipy H6), 6.92 (br, 1H, bipy H5), 2.00 (ddd, J_{HH} = 12.4, 10.2; J_{HP} = 6.2, 1H, PdCH(CN)CH$_2$), 1.66 (m, 1H, PdCH(CN)CH_2), 1.48 (s, 9H, CMe_3), 1.41 (m, 1H, PdCH(CN)-CH_2), 1.30 (s, 9H, CMe_3), 0.76 (t, J = 7, 3H, PdCH(CN)CH$_2$CH_3). ^{13}C{^{1}H} NMR (CD_2Cl_2): δ 166.9 (bipy C2), 166.2 (bipy C2), 156.3 (bipy C4), 155.7 (bipy C4), 151.3 (bipy C6), 150.1 (bipy, C6), 135.1 (d, J = 11, *o*-Ph), 133.0 (d, J = 2, *p*-Ph), 129.9 (d, J = 11, *m*-Ph), 127.6 (d, J = 53, Ph C_{ipso}), 125.1 (bipy), 123.9 (bipy), 122.6 (*C*N), 120.3 (bipy), 120.2 (bipy), 36.1 (*C*Me$_3$), 35.9 (*C*Me$_3$), 30.2 (C*Me*$_3$), 30.0 (C*Me*$_3$), 24.6 (PdCH(CN)*C*H$_2$), 15.9 (d, J = 6, Pd*C*H(CN)CH$_2$), 15.0 (PdCH(CN)CH$_2$*C*H$_3$). ^{31}P{^{1}H} NMR (CD_2Cl_2): δ 40.7 (s, PPh_3). Key ^{1}H-^{1}H COSY correlations δ/δ: 2.00 (PdCH(CN)CH$_2$)/1.66 (PdCH-(CN)CH_2); 2.00 (PdCH(CN)CH$_2$)/1.41 (PdCH(CN)CH_2); 1.66 (PdCH-(CN)CH_2)/1.41 (PdCH(CN)CH_2); 1.66 (PdCH(CN)CH_2)/0.76 (PdCH-(CN)CH$_2$CH_3); 1.41 (PdCH(CN)CH_2)/ 0.76 (PdCH(CN)CH$_2$CH_3). ESI-MS: (*t*Bu$_2$bipy)Pd{CH(CN)CH$_2$CH$_3$}(PPh$_3$)$^+$ calcd. *m*/*z* 704.2, found 704.1.

[(bim)Pd{CH(CN)CH$_2$CH$_3$}(PMe$_3$)][B(C$_6$F$_5$)$_4$] (6a). An NMR tube containing a solution of [(bim)Pd{CH(CN)CH$_2$CH$_3$}]$_n^{n+}$ (B(C$_6$F$_5$)$_4^-$ salt, **4a**, 0.013 mmol) in CD_2Cl_2 (0.6 mL) was cooled to −196 °C and PMe_3 (0.014 mmol) was added by vacuum transfer. The tube was warmed to 23 °C and vigorously agitated resulting in an off-white solution. After 5 min at 23 °C, NMR spectra showed that (bim)Pd{CH(CN)-CH$_2$CH$_3$}(PMe$_3$)$^+$ (**6a**) had formed in 90% yield. ^{1}H NMR (CD_2Cl_2): δ 7.50 (s, 1H, imidazole), 6.98 (s, 1H, imidazole), 6.94 (d, J = 1, 1H, imidazole), 6.86 (d, J = 1, 1H, imidazole), 4.17 (s, 2H, CH_2), 3.75 (s, 3H, N*Me*), 3.72 (s, 3H, N*Me*), 1.93 (m, 1H, PdCH(CN)CH$_2$), 1.53 (d, J = 11, 9H, PMe_3), 1.46 (m, 2H, PdCH(CN)CH_2), 1.03 (t, J = 7, 3H, PdCH(CN)CH$_2$CH_3). ^{13}C{^{1}H} NMR (CD_2Cl_2): δ 142.2 (imidazole C2), 141.7 (imidazole C2), 128.6 (imidazole C4), 126.8 (imidazole C4), 123.8 (*C*N), 122.8 (imidazole C5), 122.6 (d, J = 4, imidazole C5), 34.5 (N*Me*), 34.4 (N*Me*), 25.6 (PdCH(CN)*C*H$_2$), 23.2 (CH_2), 15.6 (PdCH(CN)CH$_2$*C*H$_3$), 14.8 (d, J = 35, PMe_3), 9.0 (d, J = 6, Pd*C*H-(CN)CH$_2$). ^{31}P{^{1}H} NMR (CD_2Cl_2): δ −5.3 (s, PMe_3). Key ^{1}H-^{1}H COSY correlations δ/δ: 1.93 (PdCH(CN)CH$_2$)/1.46 (PdCH(CN)CH_2); 1.46 (PdCH(CN)CH_2)/1.03 (PdCH(CN)CH$_2$CH_3). ESI−MS: (bim)Pd-{CH(CN)CH$_2$CH$_3$}(PMe$_3$)$^+$ calcd. *m*/*z* 426.1, found 426.0; B(C$_6$F$_5$)$_4^-$ calcd. *m*/*z* 679.0, found 678.7. IR (neat): ν_{CN} = 2193 cm^{-1}.

[(Tbim)Pd{CH(CN)CH$_2$CH$_3$}(PMe$_3$)][B(C$_6$F$_5$)$_4$] (6b). This species was generated in 95% yield in 5 min at 23 °C from [(Tbim)Pd{CH-(CN)CH$_2$CH$_3$}]$_n^{n+}$ (B(C$_6$F$_5$)$_4^-$ salt, **4b**, 0.018 mmol) and PMe_3 (0.018 mmol) using the procedure for **6a**. **6b** exists as two diastereomers. The diastereomer ratio was 3/1 after 5 min and did not change after 24 h at 23 °C. *NMR data for major diastereomer:* ^{1}H NMR (CD_2Cl_2): δ 7.54 (s, 1H, imidazole), 7.03 (d, J = 8, 6H, tolyl H2), 6.86 (d, J = 1, 1H, imidazole), 6.85 (s, 1H, imidazole), 6.83 (d, J = 1, 1H, imidazole), 6.62 (d, J = 8, 6H, tolyl H3), 5.86 (s, 1H, CH), 3.27 (s, 3H, N*Me*), 3.16 (s, 3H, N*Me*), 2.33 (s, 9H, tolyl Me), 1.55 (m, 1H, PdCH(CN)-CH$_2$), 1.47 (m, 2H, PdCH(CN)CH_2), 1.39 (d, J = 10, 9H, PMe_3), 1.10 (t, J = 8, 3H, PdCH(CN)CH$_2$CH_3). ^{13}C{^{1}H} NMR (CD_2Cl_2): δ 144.6 (imidazole C2), 144.5 (imidazole C2), 139.6 (tolyl C_{ipso}), 138.4 (tolyl C_{ipso}), 131.9 (tolyl C3), 129.5 (d, J = 3, imidazole C), 128.9 (tolyl C2), 126.8 (imidazole C), 126.5 (*C*N), 123.1 (d, J = 4, imidazole C), 123.0 (imidazole C), 65.3 ((tolyl)$_3$*C*), 46.2 (CH), 35.8 (N*Me*), 35.3 (N*Me*), 25.6 (PdCH(CN)*C*H$_2$), 20.9 (tolyl Me), 15.7 (PdCH(CN)-CH$_2$*C*H$_3$), 14.8 (d, J = 34, PMe_3), 9.1 (d, J = 8, Pd*C*H(CN)CH$_2$). ^{31}P-{^{1}H} NMR (CD_2Cl_2): δ −7.3 (s, PMe_3). Key ^{1}H−^{1}H COSY correlations δ/δ: 1.55 (PdCH(CN)CH$_2$)/1.47 (PdCH(CN)CH_2); 1.47 (PdCH(CN)CH_2)/1.10 (PdCH(CN)CH$_2$CH_3). Key ^{1}H−^{13}C HMQC correlations δ ^{1}H/δ ^{13}C: 1.55 (PdCH(CN))/9.1 (Pd*C*H(CN)); 1.47 (PdCH-(CN)CH_2)/25.6 (PdCH(CN)*C*H$_2$); 1.10 (PdCH(CN)CH$_2$CH_3)/15.7 (PdCH-(CN)CH$_2$*C*H$_3$). *NMR data for minor diastereomer:* ^{1}H NMR (CD_2Cl_2): δ 7.20 (s, 1H, imidazole), 7.08 (d, J = 8, 6H, tolyl H2), 6.89 (s, 1H, imidazole), 6.84 (s, 1H, imidazole), 6.80 (s, 1H, imidazole), 6.65 (d, J = 8, 6H, tolyl H3), 5.71 (s, 1H, CH), 3.19 (s, 3H, N*Me*), 3.15 (s, 3H, N*Me*), 2.33 (s, 9H, tolyl Me), 1.96 (m, 1H, PdCH(CN)CH$_2$), 1.64 (m, 2H, PdCH(CN)CH_2), 1.37 (d, J = 10, 9H, PMe_3), 1.15 (t, J = 8, 3H, PdCH(CN)CH$_2$CH_3). ^{13}C{^{1}H} NMR (CD_2Cl_2): δ 144.9 (imidazole C2), 144.0 (imidazole C2), 139.4 (tolyl C_{ipso}), 138.3 (tolyl C_{ipso}), 132.0 (tolyl C3), 129.1 (imidazole C), 129.0 (tolyl C2), 127.3 (*C*N), 127.1 (imidazole C), 123.3 (d, J = 3, imidazole C), 122.9 (imidazole C), 65.5 ((tolyl)$_3$*C*), 46.0 (CH), 36.0 (N*Me*), 35.0 (N*Me*), 25.4 (PdCH-(CN)*C*H$_2$), 20.9 (tolyl Me), 15.4 (PdCH(CN)CH$_2$*C*H$_3$), 14.8 (d, J = 34, PMe_3), 9.0 (d, J = 8, Pd*C*H(CN)CH$_2$). ^{31}P{^{1}H} NMR (CD_2Cl_2): δ

−7.7 (s, PMe_3). Key $^1H-^1H$ COSY correlations δ/δ: 1.96 (PdC*H*(CN)-CH_2)/1.64 (PdCH(CN)CH_2); 1.64 (PdCH(CN)CH_2)/1.15 (PdCH(CN)-CH_2CH_3). Key $^1H-^{13}C$ HMQC correlations δ $^1H/\delta$ ^{13}C: 1.96 (PdC*H*-(CN))/9.0 (PdC*H*(CN)); 1.64 (PdCH(CN)CH_2)/25.4 (PdCH(CN)CH_2); 1.15 (PdCH(CN)CH_2CH_3)/15.4 (PdCH(CN)CH_2CH_3). ESI−MS: (Tbim)-Pd{CH(CN)CH_2CH_3}$(PMe_3)^+$ calcd. *m*/*z* 710.3, found 710.2; $B(C_6F_5)_4^-$ calcd. *m*/*z* 679.0, found 678.7.

[($CH_2py'_2$)Pd{CH(CN)CH_2CH_3}(PMe_3)][$B(C_6F_5)_4$] (6c). This species was generated in 95% yield from [($CH_2py'_2$)Pd{CH(CN)CH_2-CH_3}]$_n^{n+}$ ($B(C_6F_5)_4^-$ salt, **4c**, 0.017 mmol) and PMe_3 (0.017 mmol) using the procedure for **6a**. **6c** exists as two isomers. The isomer ratio was 3/1 after 5 min and did not change after 24 h at 23 °C. *NMR data for major isomer:* ^1H NMR (CD_2Cl_2): δ 8.92 (s, 1H, py′ H6), 8.20 (s, 1H, py′ H6), 7.72 (d, $J = 8$, 1H, py′ H4), 7.68 (d, $J = 8$, 1H, py′ H4), 7.44 (m, *2*H, py′ H3), 4.82 (d, $J = 14$, 1H, CH_2), 4.29 (d, $J = 14$, 1H, CH_2), 2.40 (s, 3H, py′ Me), 2.34 (s, 3H, py′ Me), 1.90 (ddd, $J_{HH} = 9.2, 6.6$; $J_{HP} = 11.9$, 1H, PdC*H*(CN)CH_2), 1.53 (d, $J = 11$, 9H, PMe_3), 1.31 (m, 1H, PdCH(CN)CH_2), 1.19 (m, 1H, PdCH(CN)CH_2), 0.98 (t, $J = 7$, 3H, PdCH(CN)CH_2CH_3). $^{13}C\{^1H\}$ NMR (CD_2Cl_2): δ 153.0 (py′ C2), 151.5 (py′ C6), 150.9 (py′ C2), 149.5 (py′ C6), 141.1 (py′ C4), 141.1 (py′ C4), 135.0 (py′ C5), 134.8 (py′ C5), 126.2 (*C*N), 125.2 (py′ C3), 125.0 (d, $J = 3$, py′ C3), 46.0 (CH_2), 25.5 (PdCH(CN)CH_2), 17.9 (py′ Me), 17.6 (py′ Me), 15.1 (PdCH(CN)CH_2CH_3), 14.0 (d, $J = 35$, PMe_3), 9.4 (d, $J = 7$, PdCH(CN)CH_2). $^{31}P\{^1H\}$ NMR (CD_2Cl_2): δ −5.4 (s, PMe_3). Key $^1H-^1H$ COSY correlations δ/δ: 1.90 (PdC*H*(CN)-CH_2)/δ 1.31 (PdCH(CN)CH_2); 1.90 (PdC*H*(CN)CH_2)/1.19 (PdCH(CN)-CH_2); 1.31 (PdCH(CN)CH_2)/1.19 (PdCH(CN)CH_2); 1.31 (PdCH(CN)-CH_2)/0.98 (PdCH(CN)CH_2CH_3); 1.19 (PdCH(CN)CH_2)/0.98 (PdCH(CN)-CH_2CH_3). *NMR data for minor isomer:* ^1H NMR (CD_2Cl_2): δ 8.37 (s, 1H, py′ H6), 8.17 (s, 1H, py′ H6), 7.70 (m, 2H, py′ H4), 7.45 (m, 2H, py′ H3), 4.89 (d, $J = 14$, 1H, CH_2), 4.31 (d, $J = 14$, 1H, CH_2), 2.38 (s, 3H, py′ Me), 2.33 (s, 3H, py′ Me), 1.90 (m, 1H, PdC*H*(CN)CH_2), 1.53 (d, $J = 11$, 9H, PMe_3), 1.16 (m, 2H, PdCH(CN)CH_2), 1.01 (t, $J = 7$, 3H, PdCH(CN)CH_2CH_3). $^{13}C\{^1H\}$ NMR (CD_2Cl_2): δ 151.8 (py′ C6), 149.6 (py′ C6), 141.2 (py′ C4), 141.1 (py′ C4), 125.4 (py′ C3), 124.8 (py′ C3), 46.0 (CH_2), 24.7 (PdCH(CN)CH_2), 17.8 (py′ Me), 17.5 (py′ Me), 14.9 (PdCH(CN)CH_2CH_3), 13.4 (d, $J = 34$, PMe_3), 11.1 (PdCH(CN)CH_2). The py′ C2, C5, and *C*N resonances were not observed. $^{31}P\{^1H\}$ NMR (CD_2Cl_2): δ −6.5 (s, PMe_3). ESI−MS: (CH_2-py'_2)Pd{CH(CN)CH_2CH_3}$(PMe_3)^+$ calcd. *m*/*z* 448.1, found 447.9; $B(C_6F_5)_4^-$ calcd. *m*/*z* 679.0, found 678.7.

[(bim)Pd{CH(CN)CH_2CH_3}(CO)][$B(C_6F_5)_4$] (7a). An NMR tube containing a solution of [(bim)Pd{CH(CN)CH_2CH_3}]$_n^{n+}$ ($B(C_6F_5)_4^-$ salt, **4a**, 0.013 mmol) in CD_2Cl_2 (0.6 mL) was cooled to −196 °C and CO (0.558 mmol, corresponding to ca. 6.7 atm at 23 °C) was added. The tube was warmed to 23 °C to yield an off-white solution. After 5 min, NMR spectra showed that (bim)Pd{CH(CN)CH_2CH_3}$(CO)^+$ (**7a**) had formed quantitatively.[44] Separate resonances for free (δ 184.0) and coordinated CO are present in the ^{13}C NMR spectrum at 23 °C. ^1H NMR (CD_2Cl_2): δ 7.19 (d, $J = 1$, 1H, imidazole), 7.14 (d, $J = 1$, 1H, imidazole), 7.09 (d, $J = 1$, 1H, imidazole), 7.00 (d, $J = 1$, 1H, imidazole), 4.19 (d, $J = 18$, 1H, CH_2), 4.16 (d, $J = 18$, 1H, CH_2), 3.80 (s, 3H, N*Me*), 3.77 (s, 3H, N*Me*), 2.83 (m, 1H, PdC*H*(CN)CH_2), 1.92 (m, 2H, PdCH(CN)CH_2), 1.21 (t, $J = 7$, 3H, PdCH(CN)CH_2CH_3). $^{13}C\{^1H\}$ NMR (CD_2Cl_2): δ 174.2 (PdCO), 141.4 (imidazole C2), 140.1 (imidazole C2), 128.9 (imidazole C4), 125.8 (imidazole C4), 124.2 (*C*N), 124.0 (imidazole C5), 123.8 (imidazole C5), 35.1 (N*Me*), 34.6 (N*Me*), 29.5 (PdCH(CN)CH_2), 23.2 (CH_2), 16.4 (PdC*H*(CN)CH_2), 15.5 (PdCH(CN)CH_2CH_3). Key $^1H-^1H$ COSY correlations δ/δ: 2.83 (PdC*H*(CN)CH_2)/1.92 (PdCH(CN)CH_2); 1.92 (PdCH(CN)CH_2)/1.21 (PdCH(CN)CH_2CH_3). Key $^1H-^{13}C$ HMQC correlations δ $^1H/\delta$ ^{13}C: 2.83 (PdC*H*(CN))/16.4 (PdC*H*(CN)); 1.92 (PdCH(CN)CH_2)/29.5 (Pd-CH(CN)CH_2); 1.21 (PdCH(CN)CH_2CH_3)/15.5 (PdCH(CN)CH_2CH_3). The volatiles were removed under vacuum to yield a pale yellow solid. The solid was dried under vacuum for 10 min and dissolved in CD_2-Cl_2 (0.6 mL). NMR analysis showed that the solid was **4a**. In a separate experiment, **7a** was formed under 6.7 atm CO pressure. The CO pressure was decreased to 1 atm. NMR analysis showed that **7a** was completely converted to **4a**.

[(Tbim)Pd{CH(CN)CH_2CH_3}(CO)][$B(C_6F_5)_4$] (7b). This compound was generated quantitatively from [(Tbim)Pd{CH(CN)CH_2-CH_3}]$_n^{n+}$ ($B(C_6F_5)_4^-$ salt, **4b**, 0.018 mmol) and CO (0.558 mmol, corresponding to ca. 6.7 atm at 23 °C) using the procedure for **7a**. **7b** exists as two diastereomers. The diastereomer ratio was 4/3 after 5 min and reached a constant value of 1/1 after 2 h at 23 °C. **7b** is stable under 1 atm of CO. *NMR data for diastereomer A:* ^1H NMR (CD_2-Cl_2): δ 7.23 (d, $J = 1$, 1H, imidazole), 7.10 (d, $J = 8$, 6H, tolyl H2), 6.98 (d, $J = 1$, 1H, imidazole), 6.96 (d, $J = 1$, 1H, imidazole), 6.95 (d, $J = 1$, 1H, imidazole), 6.54 (d, $J = 8$, 6H, tolyl H3), 5.83 (s, 1H, CH), 3.30 (s, 3H, N*Me*), 3.13 (s, 3H, N*Me*), 2.41 (m, 1H, PdC*H*(CN)CH_2), 2.36 (s, 9H, tolyl Me), 1.67 (m, 2H, PdCH(CN)CH_2), 1.15 (t, $J = 7$, 3H, PdCH(CN)CH_2CH_3). $^{13}C\{^1H\}$ NMR (CD_2Cl_2): δ 173.7 (Pd−CO), 144.9 (imidazole C2), 142.5 (imidazole C2), 139.1 (tolyl C_{ipso}), 137.7 (tolyl C_{ipso}), 132.1 (tolyl C3), 129.0 (tolyl C2), 128.7 (imidazole C), 125.6 (imidazole C), 124.7 (imidazole C), 124.6 (*C*N), 123.9 (imidazole C), 66.6 ((tolyl)$_3$*C*), 45.7 (CH), 36.4 (N*Me*), 35.0 (N*Me*), 29.6 (PdCH-(CN)CH_2), 20.9 (tolyl Me), 15.6 (PdCH(CN)CH_2CH_3), 14.7 (Pd*C*H-(CN)CH_2). Key $^1H-^1H$ COSY correlations δ/δ: 2.41 (PdC*H*(CN)CH_2)/1.67 (PdCH(CN)CH_2); 1.67 (PdCH(CN)CH_2)/1.15 (PdCH(CN)CH_2CH_3). Key $^1H-^{13}C$ HMQC correlations δ $^1H/\delta$ ^{13}C: 2.41 (PdC*H*(CN))/14.7 (Pd*C*H(CN)); 1.67 (PdCH(CN)CH_2)/29.6 (PdCH(CN)CH_2); 1.15 (PdCH-(CN)CH_2CH_3)/15.6 (PdCH(CN)CH_2CH_3). *NMR data for diastereomer B:* ^1H NMR (CD_2Cl_2): δ 7.12 (d, $J = 8$, 6H, tolyl H2), 7.01 (d, $J = 1$, 1H, imidazole), 6.96 (d, $J = 1$, 1H, imidazole), 6.95 (d, $J = 1$, 1H, imidazole), 6.88 (d, $J = 1$, 1H, imidazole), 6.59 (d, $J = 8$, 6H, tolyl H3), 5.84 (s, 1H, CH), 3.35 (s, 3H, N*Me*), 3.10 (s, 3H, N*Me*), 2.58 (m, 1H, PdC*H*(CN)CH_2), 2.37 (s, 9H, tolyl Me), 1.85 (m, 2H, PdCH(CN)-CH_2), 1.23 (t, $J = 7$, 3H, PdCH(CN)CH_2CH_3). $^{13}C\{^1H\}$ NMR (CD_2-Cl_2): δ 173.7 (Pd−CO), 144.6 (imidazole C2), 142.4 (imidazole C2), 139.0 (tolyl C_{ipso}), 137.8 (tolyl C_{ipso}), 132.1 (tolyl C3), 129.1 (tolyl C2), 128.8 (imidazole C), 125.0 (imidazole C), 124.6 (imidazole C), 124.1 (*C*N), 123.8 (imidazole C), 66.5 ((tolyl)$_3$*C*), 45.8 (CH), 36.5 (N*Me*), 34.8 (N*Me*), 28.8 (PdCH(CN)CH_2), 20.8 (tolyl Me), 15.3 (PdCH(CN)-CH_2CH_3), 14.9 (Pd*C*H(CN)CH_2). Key $^1H-^1H$ COSY correlations δ/δ: 2.58 (PdC*H*(CN)CH_2)/1.85 (PdCH(CN)CH_2); 1.85 (PdCH(CN)CH_2)/1.23 (PdCH(CN)CH_2CH_3). Key ^1H-^{13}C HMQC correlations δ $^1H/\delta$ ^{13}C: 2.58 (PdC*H*(CN))/14.9 (Pd*C*H(CN)); 1.85 (PdCH(CN)CH_2)/28.8 (PdCH(CN)CH_2); 1.23 (PdCH(CN)CH_2CH_3)/15.3 (PdCH(CN)CH_2CH_3). ESI-MS: Major cation observed: [(Tbim)Pd{CH(CN)CH_2CH_3}$(CO)^+$-CO] calcd. *m*/*z* 634.2, found 634.0. IR (CD_2Cl_2, under 1 atm CO): $\nu_{CO} = 2132$ cm^{-1}.

[(bim)Pd{C(═O)CH(CN)CH_2CH_3}(CO)][$B(C_6F_5)_4$] (8a). An NMR tube containing a solution of [(bim)Pd{CH(CN)CH_2CH_3}(CO)]-[$B(C_6F_5)_4$] (**7a**, 0.013 mmol) in CD_2Cl_2 (0.6 mL) and CO (0.558 mmol, corresponding to ca. 6.7 atm at 23 °C) was maintained at 23 °C and monitored periodically by NMR. The spectra showed that **7a** was slowly converted to (bim)Pd{C(═O)CH(CN)CH_2CH_3}$(CO)^+$ (**8a**). After 2 d, the [**8a**]/[**7a**] ratio reached a constant equilibrium value of 1/3. In a similar experiment using 20 atm of CO, the equilibrium [**8a**]/[**7a**] ratio was 1/1 after 2 d. The equilibrium constant, $K_{eq} = [\mathbf{8a}][\mathbf{7a}]^{-1}P_{CO}^{-1} = 0.050(2)$ atm^{-1}, was determined by six experiments, with P_{CO} in the range of 4 to 20 atm. Data for (bim)Pd{C(═O)CH(CN)CH_2CH_3)}-$(CO)^+$: ^1H NMR (CD_2Cl_2): δ 7.07 (d, $J = 2$, 1H, imidazole), 7.06 (d, $J = 2$, 1H, imidazole), 6.91 (d, $J = 2$, 1H, imidazole), 6.83 (d, $J = 2$, 1H, imidazole), 4.27 (s, 2H, CH_2), 3.78 (s, 3H, N*Me*), 3.76 (s, 3H,

(44) The imidazole ^1H NMR resonance at δ 7.19 of complex **7a** shifts slightly upfield (<0.08 ppm), and the Pd*C*H(CN) methine ^{13}C NMR resonance at δ 16.4 shifts slightly upfield (<0.7 ppm) when excess [$HNMe_2Ph$][$B(C_6F_5)_4$] is present. These effects are attributed to partial protonation of the cyanide group of **7a** by $HNMe_2Ph^+$, which has been confirmed by control experiments in which excess $HNMe_2Ph^+$ or NMe_2Ph was added. To ensure that the system is free of excess $HNMe_2Ph^+$, a slight excess (10%) of (bim)-$PdMe_2$ (**1a**) can be used in the activation process.

N*Me*), 3.51 (m, 1H, Pd{C(═O)C*H*(CN)}), 1.91 (m, 2H, Pd{C(═O)-CH(CN)CH_2}), 1.07 (t, J = 8, 3H, Pd{C(═O)CH(CN)CH_2CH_3}). ^{13}C-{^{1}H} NMR (CD_2Cl_2): δ 212.8 (Pd{*C*(═O)CH(CN)}), 172.4 (PdCO), 142.0 (imidazole C2), 140.8 (imidazole C2), 128.6 (imidazole C4), 128.1 (imidazole C4), 127.2 (imidazole C5), 123.8 (imidazole C5), 123.3 (*C*N), 56.4 (*C*H(CN)CH_2), 35.1 (N*Me*), 34.5 (N*Me*), 23.2 (CH_2), 22.9 (CH(CN)*C*H_2), 11.3 (CH_2*C*H_3). Key ^{1}H−^{1}H COSY correlations δ/δ: 3.51 (Pd{C(═O)C*H*(CN)})/1.91 (Pd{C(═O)CH(CN)CH_2}); 1.91 (Pd{C(═O)CH(CN)CH_2})/1.07 (Pd{C(═O)CH(CN)CH_2CH_3}). Key ^{1}H-^{13}C HMQC correlations δ ^{1}H/δ ^{13}C: 3.51 (Pd{C(═O)C*H*(CN)})/56.4 (Pd{C(═O)*C*H(CN)}); 1.91 (Pd{C(═O)CH(CN)CH_2})/22.9 (Pd-{C(═O)CH(CN)*C*H_2}); 1.07 (Pd{C(═O)CH(CN)CH_2CH_3})/11.3 (Pd-{C(═O)CH(CN)CH_2*C*H_3}). The volatiles were removed under vacuum to yield a pale yellow solid. The solid was dried under vacuum for 10 min, dissolved in CD_2Cl_2, and identified as **4a** by NMR.

[(bim)Pd{CH(CNB(C_6F_5)$_3$)CH_2CH_3}(CH_2═CH_2)][B(C_6F_5)$_4$] (9a). Solid B(C_6F_5)$_3$ (8.5 mg, 0.016 mmol) was added to an NMR tube containing solid [(bim)Pd{CH(CN)CH_2CH_3}]$_n^{n+}$ (B(C_6F_5)$_4^-$ salt, **4a**, 0.016 mmol). The tube was evacuated and CD_2Cl_2 (0.6 mL) was added by vacuum transfer at −78 °C. The tube was cooled to −196 °C and CH_2═CH_2 (0.050 mmol) was condensed in via a gas bulb. The tube was maintained at 0 °C in the NMR probe for 20 min. ^{19}F NMR showed that free B(C_6F_5)$_3$ had disappeared and ^{1}H NMR spectra showed that **9a** had formed quantitatively. Exchange of free and coordinated ethylene is slow on the NMR time scale at −60 and 0 °C. **9a** decomposes at 23 °C over several hours with formation of Pd^0. ^{1}H NMR (CD_2Cl_2, −60 °C): δ 7.07 (d, J = 2, 1H, imidazole), 7.03 (s, 1H, imidazole), 6.82 (d, J = 2, 1H, imidazole), 6.71 (d, J = 2, 1H, imidazole), 5.11(br, 4H, CH_2═CH_2), 4.19 (d, J = 17.5, 1H, CH_2), 4.16 (d, J = 17.5, 1H, CH_2), 3.76 (s, 3H, N*Me*), 3.73 (s, 3H, N*Me*), 2.30 (m, 1H, PdC*H*(CN)), 1.57 (m, 2H, PdCH(CN)CH_2), 1.01 (t, J = 7, 3H, PdCH(CN)CH_2CH_3). ^{13}C-{^{1}H} NMR (CD_2Cl_2, −60 °C): δ 140.4 (imidazole C2), 139.0 (imidazole C2), 136.7(dm, J = 250, *meta* CNB(C_6F_5)$_3$), 124.2 (imidazole C), 123.8 (imidazole C), 123.2 (imidazole C), 123.0 (imidazole C), 121.6 (*C*N), 94.1 (br, coordinated CH_2═CH_2), 34.8 (N*Me*), 34.5 (N*Me*), 22.6 (PdCH(CN)*C*H_2), 22.5 (CH_2), 14.8 (PdCH(CN)CH_2*C*H_3), 8.0 (Pd*C*H(CN)). The *ortho* and *para* CNB(C_6F_5)$_3$ ^{13}C resonances are obscured by the B(C_6F_5)$_4^-$ signals. ^{19}F NMR (CD_2Cl_2, −60 °C): δ −134.9 (d, J = 17, 2F, *ortho*-CNB(C_6F_5)$_3$), −156.9 (t, J = 22, 1F, *para*-CNB(C_6F_5)$_3$), −167.0 (t, J = 22, 2F, *meta*-CNB(C_6F_5)$_3$).

[(Tbim)PdMe(CH_2═CH_2)][B(C_6F_5)$_4$] (10b). This species was generated as described previously.[17] ^{1}H NMR (CD_2Cl_2, −30 °C): δ 7.02 (d, J = 8, 6H, tolyl H2), 6.91 (s, 1H, imidazole), 6.88 (s, 1H, imidazole), 6.84 (s, 1H, imidazole), 6.61 (s, 1H, imidazole), 6.47 (d, J = 8, 6H, tolyl H3), 5.77 (s, 1H, CH), 4.34 (AA′BB′, 4H, C_2H_4), 3.23 (s, 3H, N*Me*), 3.11 (s, 3H, N*Me*), 2.31 (s, 9H, tolyl Me), 0.16 (s, 3H, PdMe).

Acknowledgment. This work was supported by Bayer Polymers (Leverkusen) and the US Department of Energy (DE-FG02-00ER15036). We thank Prof. Warren Piers, Prof. Tom Ziegler, and Dr. Thomas Weiss for helpful discussions and for sharing unpublished results prior to publication.

JA044122T